Low-spin structure of ^{156}Dy through γ-ray spectroscopy

M. A. Caprio,[1] N. V. Zamfir,[1,2,3] R. F. Casten,[1] C. J. Barton,[1,2,4] C. W. Beausang,[1] J. R. Cooper,[1,5] A. A. Hecht,[1] R. Krücken,[1,6] H. Newman,[1,7] J. R. Novak,[1] N. Pietralla,[1,8] A. Wolf,[1,2,9] and K. E. Zyromski[1]

[1]*Wright Nuclear Structure Laboratory, Yale University, New Haven, Connecticut 06520*

[2]*Clark University, Worcester, Massachusetts 01610*

[3]*National Institute for Physics and Nuclear Engineering, RO-76900 Bucharest-Magurele, Romania*

[4]*CLRC Daresbury Laboratory, Daresbury, Warrington WA4 4AD, United Kingdom*

[5]*Lawrence Livermore National Laboratory, Livermore, California 94551*

[6]*Physik Department E12, Technische Universität München, D-85748 Garching, Germany*

[7]*University of Surrey, Guilford, Surrey GU2 7XH, United Kingdom*

[8]*Institut für Kernphysik, Universität zu Köln, D-50937 Köln, Germany*

[9]*Nuclear Research Center Negev, Beer-Sheva, Israel*

(Received 30 July 2002; published 27 November 2002)

Excited states of ^{156}Dy were populated through β^+/ε decay and studied through γ-ray spectroscopy at the Yale Moving Tape Collector. Extensive data led to improved information on the electromagnetic decay properties of low-spin states and to a substantially revised level scheme. The structural observables of ^{156}Dy are compared with those of the other nearby $N=90$ isotones and to predictions of the $X(5)$ model for nuclei in the spherical-deformed transition region.

DOI: 10.1103/PhysRevC.66.054310 PACS number(s): 21.10.Re, 23.20.Lv, 27.70.+q

I. INTRODUCTION

Intriguing phenomenological observations regarding nuclei in the $N=90$ spherical-deformed shape transitional region, as well as new theoretical constructs for the understanding of these nuclei, have led to renewed interest in the $N=90$ isotonic chain. The evolution of observables across spherical-deformed transitional regions exhibits discontinuous behavior [1,2] resembling that found in phase transitions [3–5]. The $X(5)$ model recently proposed by Iachello [6], based upon the analytic solution for a square-well potential, provides a simple description of nuclei near the ''critical point'' of the spherical to axially-symmetric rotor transition.

Recent experiments performed on the $N=90$ nuclei ^{152}Sm [7–10] and ^{150}Nd [11], populating low-spin states of interest through β decay, neutron capture, and Coulomb excitation, have provided a wealth of new spectroscopic and lifetime information. The important structural signatures in transitional regions, beyond the basic yrast level properties, involve γ-ray transitions between low-spin, non-yrast levels. Reliable information on γ-ray branching ratios, multipolarities, and absolute matrix elements (or level lifetimes) is crucial. The γ-ray transitions of interest, however, often originate from weakly populated levels, are of low transition energy, or have small matrix elements. They are consequently weak from an experimental viewpoint, requiring sensitive spectroscopy for their study.

The nucleus ^{156}Dy shows marked similarities to the lower-Z $N=90$ isotones, in both level energies and transition strengths (see section IV). The yrast band level energies (Fig. 1) closely match those of ^{150}Nd, ^{152}Sm, and ^{154}Gd and are nearly identical to the $X(5)$ [6] model predictions.

Further interpretation of the structure of ^{156}Dy requires accurate information on the branching properties of the low-lying nonyrast states. The previous spectroscopic studies of ^{156}Dy, both from in-beam data and decay data, present seriously contradictory results for some of the most basic observables concerning the low-lying off-yrast states: values stated in the literature for the intensities of some branching transitions from the lowest excited 2^+ and 4^+ states [13] disagree by factors of five or more, and values for others have uncertainties which are too large for useful analysis.

The purpose of this study is to provide reliable intensity information on transitions depopulating low-lying levels in ^{156}Dy populated in β decay. The present experiment provides high-statistics γ-ray coincidence spectroscopy data, allowing many of the ambiguities (e.g., contaminant transitions, unresolved doublets) inherent to singles studies to be largely avoided. Substantially improved measurements of the branching properties of low-lying levels are obtained, resolving the outstanding conflicts in the literature, and it is found that much of the previous level scheme (above ~1200 keV) is in error. Following a summary of the experimental methods (Sec. II), the spectroscopic results are presented (Sec. III) and discussed in the context both of the neighboring nuclei

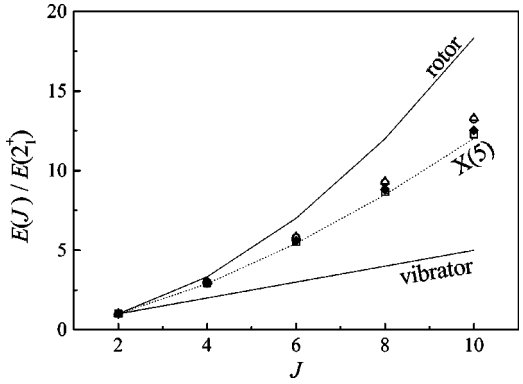

FIG. 1. Yrast band level energies, normalized to the 2^+ band member, for the $N=90$ isotones ^{150}Nd (□), ^{152}Sm (○), ^{154}Gd (△), and ^{156}Dy (◆). The rotor, $X(5)$, and vibrator predictions are shown for comparison. (Figure from Ref. [12].)

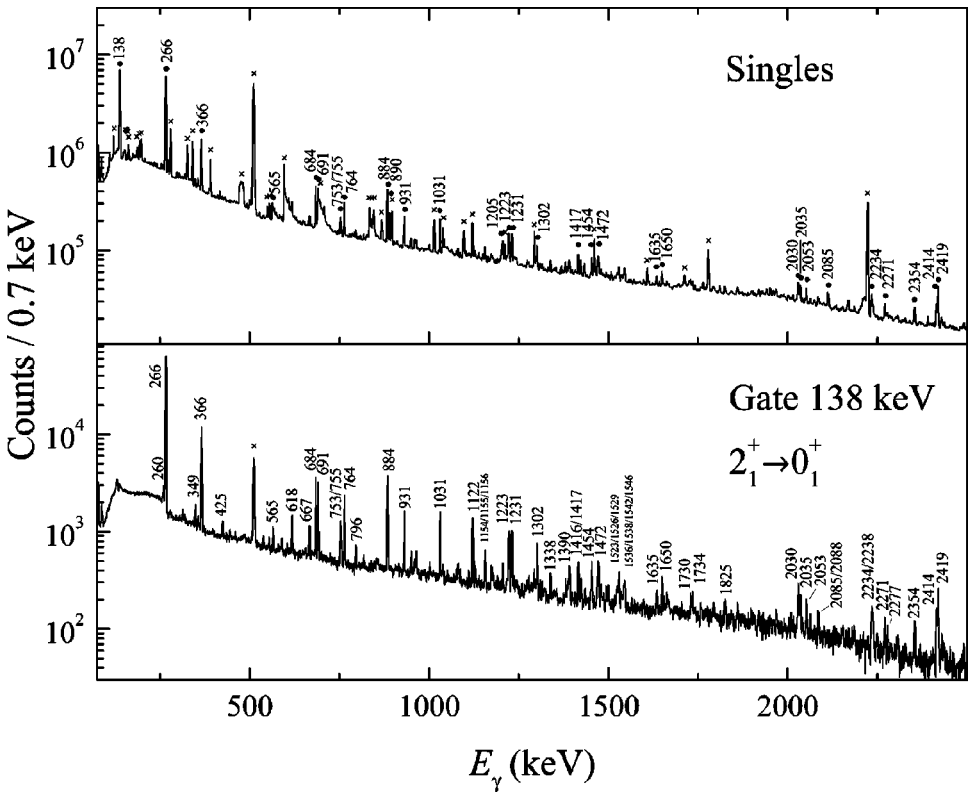

FIG. 2. (Top) Clover singles spectrum. Transitions from ^{156}Dy are marked with a circle (●). Contaminant lines (from ^{157}Ho, ^{157}Dy, room or neutron-induced background, and positron annihilation) are indicated with a cross (×). (Bottom) Clover-clover coincidence spectrum gated on the 138-keV $2_1^+ \rightarrow 0_1^+$ transition. Annihilation radiation is indicated with a cross (×).

and model predictions (Sec. IV). Preliminary results of this work were reported in Ref. [14].

II. EXPERIMENT AND TECHNIQUES

A. Decay experiment

The nucleus ^{156}Dy was populated in β^+/ε decay and studied through γ-ray coincidence spectroscopy at the Yale Moving Tape Collector [15,16]. Parent ^{156}Er nuclei were produced through the reaction ^{148}Sm(^{12}C,4n)^{156}Er at a beam energy of 73 MeV, using an ~10-pnA beam provided by the Yale ESTU tandem accelerator incident upon a 1.8-mg/cm^2 96%-isotopically-enriched target. The recoil product nuclei were embedded into a 16 mm Kapton tape. The primary beam nuclei were stopped by a 3-mm diameter gold plug 5 cm downstream of the target prior to reaching the tape. In contrast, the fusion-evaporation product nuclei, which were emitted from the target with a much wider angular distribution, largely bypassed the plug [15], reaching the tape with ~75% geometrical acceptance. The tape was advanced at 1-h intervals, carrying the collected activity to a shielded detector area.

The ^{156}Er parent nucleus decays with a 19.5-min half life to ^{156}Ho [$J^\pi=(4^+)$], which in turn decays with a 56-min half life to ^{156}Dy [13]. Two-step decay was chosen to enhance the population of low-spin off-yrast states in ^{156}Dy, as beta decay from the 0^+ ground state of ^{156}Er avoids population of β-decaying high spin isomeric states in ^{156}Ho.

Three Compton-suppressed segmented YRAST Ball clover HPGe detectors [17] and one low-energy photon spectrometer (LEPS) detector were positioned about the source in close geometry, with an array photopeak efficiency of 1.1% at 1.3 MeV and dynamic range extending from ~35 keV to 2650 keV. Data were acquired in event mode with a singles (or higher fold) trigger, using a FERA/VME acquisition system [17]. The experiment, which lasted 125 h, yielded 7.2 $\times 10^8$ clover singles events and 1.7×10^7 clover-clover coincidence pairs.

The combined clover singles spectrum from the experiment is shown in Fig. 2 (top). Some contamination from the neighboring mass chains (primarily $A=157$) is seen to be present. An example of a gated spectrum is given in Fig. 2 (bottom).

B. Determination of transition intensities

The nucleus ^{156}Dy was populated in this experiment at a Q_ε value of ~5 MeV [13], resulting in the production of several hundred identifiable transitions, many of them yielding overlapping or unresolved peaks in the singles spectra. Measurements of intensities from such singles data are therefore not always reliable, and the singles data could only provide meaningful intensity information for a handful of the strongest transitions.

In comparison, the high-statistics coincidence data obtained in this experiment provide not only information on the *placement* of transitions in the level scheme, but also allow for reliable measurement of γ-ray transition *intensities*, from peak areas in clean gated spectra. When the transition x of interest directly feeds a level which decays by a γ radiation b, for which the intensity branching fraction B_b is known, then the absolute intensity I_x is determined from

$$G_{b:x}=NI_xB_b\varepsilon(E_b,E_x), \quad (1)$$

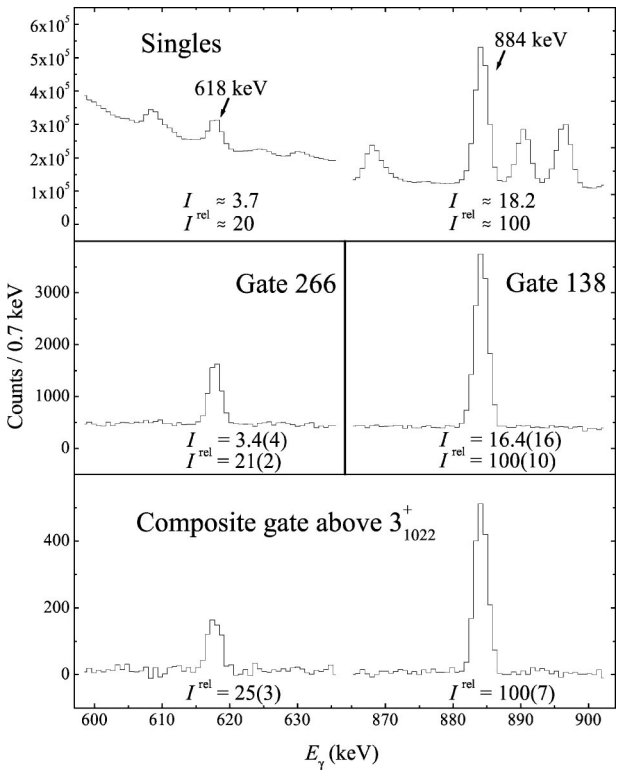

FIG. 3. Comparison of the different sources of intensity information for the 618- and 884-keV branches from the 3^+ level at 1022 keV. The spectra are (top) from singles, (middle) gated below the branch of interest, or (bottom) gated on transitions feeding the 3^+ level. The composite spectrum on the bottom is gated on 655-, 819-, 1081-, 1301-, 1310-, and 1386-keV transitions.

where $G_{b:x}$ is the number of detected coincidences between b and x from a gated spectrum, and $\varepsilon(E_b,E_x)$ is the coincidence efficiency of the array for a pair of transitions of these energies (see below). The normalization constant N is simply the same as for the singles data, $S_x = NI_x\varepsilon(E_x)$, and in this paper all intensities are normalized to the $2^+_1 \rightarrow 0^+_1$ transition intensity ($I_{138} \equiv 100$). The branching fraction B_b is calculated from known intensities as $B_b = I_b/(\Sigma_i I_i + \Sigma_i I_i^{ce})$, where the sums are over all γ-ray and conversion electron transitions depopulating the level.

The *relative* intensities of two branches x and y from a level can also be obtained from a spectrum gated on a transition a feeding the level, according to

$$\frac{G_{a:x}}{G_{a:y}} = \frac{I_x\varepsilon(E_a,E_x)}{I_y\varepsilon(E_a,E_y)}. \qquad (2)$$

Intensities can only be measured in this way if there exist one or more strong discrete feeding transitions to the level, and this method therefore tends to be useful only for levels low in the excitation spectrum. This method in most cases provides lower statistics than can be obtained by gating below the transition of interest—the intensity flow below the transition of interest is typically concentrated in one or two strong branches, but the intensity flow feeding the transition of interest is usually diluted among several weak transitions or may come from direct β feeding. A gate on a feeding transition cannot give absolute intensities unless the absolute intensity of one branch is known (to provide a normalization).

The relative quality of these different sources of intensity information is illustrated in Fig. 3, which shows the data used in the measurement of the intensities of the 617- and 884-keV branches from the 3^+ level at 1022 keV. The intensities deduced by the different methods are compatible to within the uncertainties (Fig. 3).

In the present paper, all intensity values are deduced from coincidence data. Information was extracted from coincidences both with feeding transitions and with transitions below the transition of interest whenever possible. In cases in which both methods yield intensity measurements with comparable uncertainties, a weighted average is used. The singles data were used primarily to provide corroboration of these intensities and to deduce limits on the intensities of certain unobserved transitions.

All intensity measurements rely upon an accurate knowledge of the array efficiency. The coincidence efficiency of an array of detectors is approximately the sum of the pairwise products of efficiencies of the individual array elements. Deviations from this ideal coincidence efficiency occur, however, at low γ-ray energies, since electronic timing jitter and walk can cause the signals from two coincident γ rays to fall outside the acquisition system's timing acceptance. In general, the efficiency for detection of two coincident γ rays is thus

$$\varepsilon(E_x,E_y) = w(E_x,E_y)\sum_{i,j(i\neq j)}\varepsilon_i(E_x)\varepsilon_j(E_y), \qquad (3)$$

where the sum is over individual detectors i and j, and where $w(E_x,E_y)$ is the empirically calibrated attenuation of efficiency due to such time ''windowing'' effects. For the array used in this experiment, the coincidence efficiency was verified using 35 known coincidences in ^{152}Sm and ^{152}Gd from ^{152}Eu calibration source decay [18]. Use was also made of ''internal'' calibrator coincidences from the ^{156}Dy data involving transitions in the yrast cascade, since for these transitions the branching fractions depend only upon $E2$ internal conversion coefficients, which are reliably known from atomic physics. The array exhibited an attenuation factor of $w \approx 0.65$ for γ-ray energies of $\sim$100 keV and reached ideal efficiency, $w \approx 1$, for energies above $\sim$300 keV.

Deviations from ideal coincidence efficiency also occur as a result of angular correlations between the emitted γ rays. For the clover detector pair angles used in the present experiment (approximately 110°–125°), the effect on the γ-ray intensity measurement is $\sim$24% for a spin 0-2-0 cascade and substantially smaller ($\lesssim$5%) for other common cascades. Since reliable multipolarity information is not consistently available, intensities given in this paper are not corrected for angular correlation effects.

TABLE I. Branching properties of levels populated in ^{156}Dy. Both absolute (in β decay) and relative intensities are given for γ-ray transitions depopulating the levels, and these intensities are compared with literature values [13] where available. Intensity limits are given for many unobserved transitions, in which case the approximate transition energy expected from the level energy difference is shown in brackets. (Transitions on which limits were placed include spin-allowed but unobserved transitions between low-lying levels relevant to the structural interpretation of the nucleus and presently-unobserved transitions which were reported to have been observed in the prior literature.)

Transition				Experiment			Literature	
J_i^π [a]	E_i (keV)	J_f^π	E_f (keV)	E_γ (keV)	I	$I^{\rm rel}$	I [b]	$I^{\rm rel}$ [c]
2^+	137.80(10)	0^+	0.00	137.80(10)	100(7)	100(7)	100	100
4^+	404.18(14)	2^+	137.80	266.38(10)	127(6)	100(5)	107.1(11)	100
0^+	675.6(2)	2^+	137.80	537.8(2)	0.86(12)	100(15)	0.53(7)	100
6^+	770.40(17)	4^+	404.18	366.22(12)	27.9(16)	100(6)	21.0(2)	100
2^+	828.66(15)	0^+	0.00	[829]	$<$0.4	$<$4		16(18), not obs.
		2^+	137.80	690.86(13)	10.4(5)	100(5)	8.46(13)	100(2)
		4^+	404.18	424.5(2)	1.12(6)	10.8(5)	0.77(13)	9(2)
		0^+	675.6	[153]	$<$0.07	$<$0.7	0.19[d]	36(7), 1.9[d,e]
2^+	890.50(11)	0^+	0.00	890.44(12)	5.9(9)	100(6)	5.21(8)	100(2)
		2^+	137.80	752.67(15)	3.3(3)	56(5)	3.05(18)	59(3)
		4^+	404.18	486.4(3)	0.50(8)	8.5(10)	0.31(12)	6.0(23)
		0^+	675.6	[214]	$<$0.05	$<$0.8		
		2^+	828.66	[62]	$<$0.06	$<$1.0	0.05[d]	0.9[d]
3^+	1022.10(14)	2^+	137.80	884.30(10)	16.4(16)	100(7)	13.86(11)	100.0(8)
		4^+	404.18	617.88(12)	3.6(4)	22(2)	2.68(5)	19.3(4)
		2^+	828.66	[193]	$<$0.07	$<$0.4		
		2^+	890.50	[131]	$<$0.08	$<$0.5	0.48[d]	3.5[d,f]
4^+	1088.28(14)	2^+	137.80	950.5(2)	1.2(2)	9.0(15)	1.39(6)	13.2(6)
		4^+	404.18	684.10(10)	13.3(9)	100(7)	10.54(14)	100.0(13)
		6^+	770.40	317.9(2)	0.27(4)	2.0(3)	0.33(13)	3.1(12)
		2^+	828.66	259.59(15)[g]	1.46(13)	11.0(10)		45(14),[h] 11(2),[h] not obs.
		2^+	890.50	[197]	$<$0.19	$<$1.4		
		3^+	1022.10	[66]	$<$0.3	$<$2		
4^+	1168.4(2)	2^+	137.80	1030.7(2)	7.7(4)	86(4)	6.19(9)	89.1(13)
		4^+	404.18	764.12(13)	9.0(5)	100(6)	6.91(7)	100.0(10)
		6^+	770.40	397.9(2)[g]	0.21(5)	2.3(6)		557(90),[i] not obs.
		2^+	828.66	[340]	$<$0.17	$<$1.9		
		2^+	890.50	277.96(18)	0.71(7)	7.9(8)	0.87(9)	12.5(13)
		3^+	1022.10	[146]	$<$0.2	$<$3	0.11[d]	530(60),[j] 1.7[d]
		4^+	1088.28	[80]	$<$0.3	$<$3	[0.6][k]	[9][k]
8^+	1215.6(2)[l]	6^+	770.40	445.23(17)[g]	0.37(3)	100(8)		100
5^+	1335.51(18)	4^+	404.18	931.35(16)	7.2(4)	100(6)	5.83(6)	100.0(10)
		6^+	770.40	565.07(17)	1.15(6)	16.0(8)	1.25(5)	21.4(9)
		3^+	1022.10	313.4(2)	0.66(5)	9.2(7)	0.68(13)	11.7(22)
		4^+	1088.28	[247]	$<$0.2	$<$3		
		4^+	1168.4	[167]	$<$0.3	$<$4	0.66[d]	11[d]
3^-	1368.53(18)	2^+	137.80	1230.72(14)	5.3(5)	100(10)	4.20(13)	100(3)
		4^+	404.18	964.36(18)	1.51(12)	29(2)	1.22(8)	29(2)
		2^+	828.66	[540]	$<$0.12	$<$2		
		2^+	890.50	[478]	$<$0.13	$<$3		
		3^+	1022.10	[346]	$<$0.10	$<$1.9		
		4^+	1088.28	[280]	$<$0.19	$<$4		
		4^+	1168.4	[200]	$<$0.2	$<$4		
(2^+)[m]	1382.3(2)[l,n]	0^+	0.00	[1382]	$<$0.6	$<$207		
		2^+	137.80	[1245]	$<$0.9	$<$314		

TABLE I. (*Continued.*)

Transition				Experiment			Literature	
J_i^π [a]	E_i (keV)	J_f^π	E_f (keV)	E_γ (keV)	I	I^{rel}	I [b]	I^{rel} [c]
		4^+	404.18	[978]	<0.4	<150		
		0^+	675.6	706.74(16)[o]	0.14(2)	50(7)		
		2^+	828.66	553.7(2)[o]	0.28(3)	100(11)		
		2^+	890.50	491.6(3)[o]	0.23(6)	82(21)		
		3^+	1022.10	360.7(12)[o,p]	0.11(4)	39(14)		
		4^+	1088.28	[294]	<0.11	<39		
		4^+	1168.4	[214]	<0.2	<71		
6^+	1437.28(17)	4^+	404.18	1033.2(3)[g]	0.65(13)	34(7)		16(8)
		6^+	770.40	666.88(15)	1.92(10)	100(5)	2.07(9)	100(4)
		4^+	1088.28	348.96(14)	1.41(7)	73(4)	1.46(8)	71(5)
		4^+	1168.4	[268]	<0.4	<20		
		8^+	1215.6	[222]	<0.11	<6		
		5^+	1335.51	[101]	<0.7	<37		
(?)	1476.10(16)[q]	2^+	137.80	1338.31(17)[o]	1.11(11)	100(10)		
		2^+	890.50	585.6(2)[o]	0.35(7)	32(6)		
(2^+)[m]	1515.0(2)[q]	4^+	404.18	1111.2(6)[o]	0.53(13)[r]	100(25)		
		0^+	675.6	839.3(2)[o]	0.20(2)	37(4)		
		2^+	890.50	624.4(3)[o]	0.11(5)	21(9)		
6^+	1525.3(2)[l,s]	4^+	404.18	[1121]	<3[t]	<149[t]		⩽52
		6^+	770.40	754.9(2)[g]	1.75(11)[t]	100(6)[t]		27(14)
		4^+	1088.28	[437]	<0.13[t]	<7[t]		
		4^+	1168.4	356.5(3)[g]	0.53(5)[t]	30(3)[t]		43(9)
		5^+	1335.51	[190]	<0.2	<13		100(5)[u]
(5^-)	1526.0(2)	4^+	404.18	1121.8(2)	8.2(8)[t]	100(10)[t]	6.54(11)	100.0(17)
		6^+	770.40	[755]	<0.6[t]	<7[t]	1.39(11)	21.2(17)
		4^+	1088.28	437.6(6)[o,p]	0.08(6)[t]	1.0(7)[t]		
		4^+	1168.4	[357]	<0.2[t]	<3[t]	0.42(8)	6.4(12)
$(3)^-$	1609.4(2)	0^+	0.00	[1609]	<1.3	<52	0.14(3)	6.5(14)
		2^+	137.80	1471.5(2)	2.5(3)[r]	100(12)	2.17(8)	100(4)
		4^+	404.18	1205.2(2)	1.27(11)	51(4)	0.97(9)	45(4)
(?)	1624.6(2)[q]	2^+	137.80	1486.4(7)[o]	0.54(16)	55(16)		
		2^+	828.66	796.03(15)[o]	0.98(6)	100(6)		
		4^+	1168.4	456.2(8)[o]	0.09(3)	9(3)		
$(4)^+$	1627.5(2)	4^+	404.18	1223.36(18)	5.6(4)	100(7)	4.75(13)	100(3)
		3^+	1022.10	605.5(3)	0.36(7)	6.4(13)	0.47(9)	10(2)
		4^+	1168.4	458.9(4)[o]	0.20(6)	3.6(11)		
				[178][v]	<0.07[w]	<1.2		⩽133(43)[x]
(4^+)[m]	1677.2(2)[q]	4^+	404.18	1272.8(3)[o]	0.32(8)	62(15)		
		6^+	770.40	907.2(4)[o]	0.14(5)	29(4)		
		2^+	828.66	848.2(5)[o]	0.12(5)	23(10)		
		2^+	890.50	786.1(5)[o,p]	0.10(3)	19(6)		
		3^+	1022.10	654.9(4)[o]	0.33(9)	63(17)		
		4^+	1088.28	588.88(14)[o]	0.52(4)	100(8)		
(?)	1679.9(8)[q]	2^+	137.80	1542.1(8)[o]	0.80(16)[y]	100(20)		
		2^+	828.66	851.0(12)[o,p]	0.07(4)	9(5)		
7^+	1728.7(5)[l]	6^+	770.40	958.3(8)[g]	0.22(7)[r]	100(32)		100(10)
		5^+	1335.51	393.2(6)[g]	0.09(4)	41(18)		52(8)
(?)	1772.4(10)[q]	2^+	137.80	1634.6(10)[o]	1.1(3)[r]	100(27)		
(?)	1794.6(2)[q]	4^+	404.18	1390.33(17)[o]	2.07(12)	100(6)		
		6^+	770.40	1024.6(6)[o]	0.12(5)	6(2)		

TABLE I. (*Continued.*)

Transition				Experiment			Literature	
J_i^{π} [a]	E_i (keV)	J_f^{π}	E_f (keV)	E_γ (keV)	I	I^{rel}	I [b]	I^{rel} [c]
7^-	1809.8(3)[l]	6^+	770.40	1039.3(2)[g]	0.33(5)	100(15)		observed[z]
		8^+	1215.6	594.9(6)[g]	0.047(13)	14(4)		observed[z]
(?)	1840.1(2)[q]	4^+	404.18	1435.7(5)[o]	0.47(9)	66(23)		
		2^+	828.66	1011.7(2)[o]	0.10(3)	14(4)		
		2^+	890.50	949.60(16)[o]	0.71(5)	100(7)		
		3^+	1022.10	818.1(2)[o]	0.26(6)	37(8)		
		4^+	1168.4	671.2(2)[o]	0.18(4)	25(6)		
(?)	1857.82(17)[q]	4^+	404.18	1453.65(15)[o]	2.5(3)	100(12)		
		6^+	770.40	1087.40(16)[o]	0.62(4)	24.8(16)		
		4^+	1168.4	688.9(5)[o,p]	0.15(9)	6(4)		
(?)	1878.8(6)[q]	2^+	137.80	1741.5(7)[o]	0.36(9)	64(16)		
		4^+	404.18	1474.2(4)[o]	0.56(14)	100(25)		
		2^+	828.66	1049.6(15)[o,p]	0.12(5)	21(9)		
		2^+	890.50	988.7(5)[o,p]	0.14(3)	25(5)		
(6)	1898.5(2)[l,aa]	6^+	770.40	1128.07(15)[g]	0.89(5)	100(6)		100(5)
		5^+	1335.51	562.6(5)[o]	0.12(5)	13(6)		
		$(4)^+$	1627.5	[271]	<0.16	<18		$\leqslant 88$
(?)	1930.0(5)[q]	2^+	137.80	1791.9(9)[o]	0.50(18)	78(28)		
		4^+	404.18	1526.1(6)[o]	0.64(16)	100(25)		
(?)	1933.6(2)[q]	4^+	404.18	1529.4(2)[o]	1.52(13)	100(9)		
		3^+	1022.10	911.5(6)[o]	0.15(4)	10(3)		
		4^+	1088.28	845.3(3)[o]	0.11(2)	7.2(13)		
(?)	1942.9(3)[q]	4^+	404.18	1538.0(12)[o,p]	0.41(13)	121(38)		
		6^+	770.40	1172.5(16)[o,p]	0.20(6)	59(19)		
		4^+	1088.28	854.6(3)[o]	0.34(5)	100(15)		
(?)	1950.0(2)[q]	4^+	404.18	1545.8(2)[o]	1.44(8)	100(6)		
(?)	2003.0(3)[q]	4^+	404.18	1598.7(5)[o]	0.25(7)	100(28)		
		2^+	828.66	1174.5(8)[o]	0.22(8)	88(32)		
		4^+	1088.28	914.6(3)[o]	0.14(5)	56(20)		
(?)	2058.6(2)[q]	3^+	1022.10	1036.4(2)[o]	0.32(6)	100(19)		
		4^+	1088.28	970.4(18)[o,p]	0.06(4)	19(13)		
		4^+	1168.4	890.2(4)[o]	0.27(10)	84(31)		
		5^+	1335.51	722.3(7)[o]	0.13(4)	41(13)		
(?)	2085.1(3)[q]	6^+	770.40	1314.7(2)[o]	0.52(5)	100(10)		
2^+	2089.9(3)	0^+	0.00	[2089]	<0.6	<144	0.31(13)	27(12)
		2^+	137.80	1952.3(9)[p]	0.24(10)	56(23)	0.29(4)	26(4)
		4^+	1088.28	1001.7(3)[o]	0.43(6)	100(14)		
		4^+	1168.4	921.2(3)	0.26(6)	60(14)	0.14(6)	12(5)
				[796][v]			1.13(4)	100(4)
(?)	2103.3(3)[q]	3^+	1022.10	1081.2(4)[o]	0.64(5)	100(8)		
		4^+	1168.4	935.0(4)[o]	0.19(6)	30(9)		
		5^+	1335.51	767.8(4)[o]	0.16(4)	25(6)		
(?)	2164.3(4)[q]	4^+	404.18	1760.1(4)[o]	0.31(9)	100(29)		
		6^+	770.40	1393.9(7)[o,p]	0.09(4)	29(12)		
(?)	2183.8(4)[q]	2^+	828.66	1355.1(4)[o]	0.21(5)	100(23)		
		2^+	890.50	1293.0(5)[o,p]	0.14(8)	67(38)		
		4^+	1088.28	1095.9(5)[o,p]	0.10(6)	48(29)		
(?)	2193.5(3)[q]	6^+	770.40	1423.3(6)[o]	0.16(6)	47(18)		
		5^+	1335.51	858.0(3)[o]	0.34(5)	100(15)		

TABLE I. (*Continued.*)

Transition				Experiment			Literature	
J_i^{π} [a]	E_i (keV)	J_f^{π}	E_f (keV)	E_γ (keV)	I	I^{rel}	I [b]	I^{rel} [c]
(?)	2199.7(3)[q]	4^+	404.18	1795.6(5)[o]	0.42(15)	100(36)		
		3^+	1022.10	1177.6(2)[o]	0.29(5)	69(12)		
		4^+	1168.4	1031.8(8)[o]	0.11(3)[r]	26(7)		
		5^+	1335.51	863.3(10)[o]	0.10(4)	24(10)		
		(?)	1476.10	723.5(4)[o]	0.14(4)	33(10)		
(?)	2207.4(5)[q]	3^+	1022.10	1185.6(5)[o]	0.22(4)	100(18)		
		5^+	1335.51	871.6(5)[o]	0.18(5)	82(23)		
(?)	2220.4(4)[q]	6^+	770.40	1450.0(3)[o]	0.22(6)[r]	100(27)		
(?)	2228.9(5)[q]	4^+	404.18	1824.7(5)[o]	0.63(9)	100(14)		
(?)	2230.9(4)[q]	6^+	770.40	1460.5(3)[o]	0.22(4)	100(18)		
(?)	2244.7(3)[q]	4^+	404.18	1840.5(8)[o,p]	0.22(9)	15(6)		
		2^+	828.66	1415.9(2)[o]	1.50(9)	100(6)		
		2^+	890.50	1354.1(2)[o]	0.41(5)	27(3)		
		3^+	1022.10	1222.8(3)[o]	0.37(8)	25(5)		
		4^+	1088.28	1156.4(3)[o]	0.32(7)	21(5)		
		4^+	1168.4	1076.2(5)[o]	0.42(8)	28(5)		
		(?)	1624.6	620.1(8)[o]	0.10(3)	7(2)		
(?)	2264.1(6)[q]	4^+	404.18	1860.1(5)[o]	0.81(13)	100(16)		
		3^+	1022.10	1241.2(6)[o,p]	0.15(6)	19(7)		
		4^+	1168.4	1094.8(10)[o,p]	0.15(5)	19(6)		
(?)	2270.0(4)[q]	6^+	770.40	1499.6(3)[o]	0.62(9)	100(15)		
(?)	2293.4(4)[q]	4^+	404.18	1888.8(15)[o,p]	0.27(10)	71(26)		
		6^+	770.40	1523.0(3)[o]	0.38(6)	100(16)		
(?)	2300.1(4)[q]	3^+	1022.10	1278.0(3)[o]	0.52(14)	100(27)		
4^+	2307.4(3)	2^+	137.80	[2169]	$<$0.4	$<$39	0.31(4)	14(2)
		4^+	404.18	1902.5(5)	0.42(10)	46(11)	0.48(6)	22(3)
		6^+	770.40	1536.0(4)	0.49(8)	53(9)	0.57(8)	26(4)
		2^+	828.66	1478.7(2)	0.28(3)	30(3)	0.66(8)	40(4)
		2^+	890.50	1416.8(2)	0.92(10)	100(11)	2.21(4)	100(2)
		3^+	1022.10	1285.4(4)[o]	0.18(7)	20(8)		
		4^+	1088.28	1218.9(5)[o]	0.39(10)	42(10)		
		4^+	1168.4	1139.0(6)[o]	0.32(9)	35(10)		
		3^-	1368.53	939.2(11)[o]	0.17(6)	18(7)		
		$(4)^+$	1627.5	[680]	$<$0.10	$<$11	0.48(10)	22(5)
(?)	2323.6(2)[q]	2^+	137.80	2185.6(6)[o]	0.31(10)	12(4)		
		4^+	404.18	1919.8(4)[o]	0.61(13)	24(5)		
		2^+	828.66	1494.5(5)[o]	0.29(7)	11(3)		
		2^+	890.50	1432.8(2)[o]	1.00(10)	39(4)		
		3^+	1022.10	1301.5(4)[o]	2.58(14)	100(5)		
		4^+	1088.28	1235.3(2)[o]	0.43(9)	17(3)		
		4^+	1168.4	1155.3(2)[o]	1.26(9)	49(3)		
		3^-	1368.53	955.4(4)[o]	0.19(4)	7.4(16)		
(?)	2331.7(3)[q]	3^+	1022.10	1309.7(4)[o]	0.37(8)	100(22)		
		4^+	1168.4	1163.1(6)[o,p]	0.10(5)	27(14)		
		5^+	1335.51	996.1(4)[o]	0.14(5)	37(14)		
(?)	2342.6(3)[q]	4^+	1168.4	1174.2(2)[o]	0.42(7)	100(17)		
(?)	2372.1(3)[q]	2^+	137.80	2234.2(4)[o]	1.7(4)	100(23)		
		4^+	404.18	1967.9(3)[o]	0.59(16)	35(9)		
(?)	2385.6(3)[q]	3^+	1022.10	1363.4(7)[o,p]	0.08(3)	32(12)		
		4^+	1168.4	1217.2(3)[o]	0.25(7)	100(28)		

TABLE I. (*Continued.*)

Transition				Experiment			Literature	
J_i^{π} [a]	E_i (keV)	J_f^{π}	E_f (keV)	E_γ (keV)	I	I^{rel}	I [b]	I^{rel} [c]
		5^+	1335.51	1050.0(5)[o]	0.11(3)	44(12)		
(?)	2408.7(4)[bb]	2^+	137.80	2271.0(2)[o]	0.88(13)	100(15)		
		4^+	404.18	2003.7(7)[p]	0.34(10)	39(11)	0.24(5)	36(7)
		2^+	828.66	1580.3(4)[o]	0.11(3)	13(3)		
		2^+	890.50	1518.7(3)[o]	0.25(7)	28(8)		
		3^+	1022.10	1386.3(2)	0.67(6)	76(7)	0.67(8)	100(12)
		4^+	1088.28	1320.3(15)	0.12(5)	14(6)	0.31(5)	46(7)
		4^+	1168.4	1241.3(12)[o,p]	0.14(6)	16(7)		
		3^-	1368.53	1040.0(7)[o]	0.11(4)	13(5)		
				[880][v]			0.66(8)	99(12)
		(?)	2103.3	304.6(7)[o,p]	0.10(3)	11(3)		
(?)	2418.9(6)[q]	4^+	404.18	2014.9(6)[o]	0.42(10)	100(24)		
		6^+	770.40	1648.1(7)[o,p]	0.19(6)	45(14)		
(?)	2433.8(2)[q]	4^+	404.18	2029.70(18)[o]	2.17(16)	100(7)		
		6^+	770.40	1663.3(2)[o]	0.52(10)	24(5)		
		4^+	1088.28	1345.6(3)[o]	0.19(5)	9(2)		
		(5^-)	1526.0	908.0(10)[o,p]	0.19(6)	9(3)		
(?)	2439.2(2)[q]	4^+	404.18	2035.0(2)[o]	1.7(2)	100(12)		
		6^+	770.40	1668.7(2)[o]	0.32(7)	19(4)		
		4^+	1088.28	1351.3(6)[o,p]	0.10(4)	6(2)		
(?)	2445.2(3)[q]	2^+	137.80	2307.4(8)[o]	0.27(11)	40(16)		
		3^+	1022.10	1423.0(2)[o]	0.68(9)	100(13)		
		5^+	1335.51	1110.7(7)[o,y]	0.29(6)	43(9)		
		(?)	1624.6	820.9(6)[o,p]	0.08(2)	12(3)		
		$(4)^+$	1627.5	818.7(4)[o,p]	0.19(5)	28(7)		
(?)	2489.5(5)[q]	4^+	404.18	2085.4(5)[o]	0.49(10)	100(20)		
		3^+	1022.10	1467.1(8)[o]	0.10(5)	20(10)		
		5^+	1335.51	1154.4(8)[o,p]	0.14(6)	29(12)		
(?)	2492.0(3)[q]	2^+	137.80	2354.1(2)[o]	0.90(8)	100(9)		
		4^+	404.18	2088.2(6)[o]	0.37(15)	41(17)		
		3^+	1022.10	1469.9(5)[o]	0.19(6)	21(7)		
		4^+	1168.4	1323.2(4)[o]	0.17(5)	19(6)		
(?)	2516.6(7)[cc]	0^+	675.6	[1841]	<0.03	<17	0.14(3)	19(4)
		2^+	828.66	1688.2(15)[p]	0.07(5)	32(25)	0.15(7)	20(9)
		2^+	890.50	1626.8(6)[p]	0.16(6)	80(30)	0.18(3)	24(4)
		3^+	1022.10	1493.8(10)	0.20(5)	100(25)	0.74(7)	99(9)
		4^+	1168.4	1348.9(5)	0.19(5)	95(25)	0.10(8)	13(11)
				[1297][v]			0.75(5)	100(7)
		3^-	1368.53	[1148]	<0.15	<75	0.12(5)	16(7)
		$(3)^-$	1609.4	[907]	<0.10	<50	0.29(5)	39(7)
(?)	2572.0(5)[q]	4^+	404.18	2168.9(7)[o,p]	0.23(8)	100(35)		
		$(4)^+$	1627.5	944.3(4)[o]	0.15(3)	65(13)		
(?)	2594.3(4)[q]	3^+	1022.10	1572.0(5)[o]	0.13(5)	62(25)		
		4^+	1168.4	1425.9(4)[o]	0.20(5)	100(25)		
		5^+	1335.51	1259.1(7)[o]	0.19(8)	95(40)		
(?)	2642.5(3)[q]	4^+	404.18	2238.3(2)[o]	0.77(13)	100(17)		
(?)	2653.4(6)[q]	4^+	404.18	2249(2)[o,p]	0.32(15)	100(47)		
		2^+	828.66	1824.7(6)[o]	0.20(5)	63(16)		
(?)	2757.8(6)[q]	3^+	1022.10	1735.7(5)[o]	0.18(5)	100(28)		
(?)	2788.1(9)[q]	8^+	1215.6	1572.5(8)[o]	0.08(2)	100(25)		

TABLE I. (*Continued.*)

Transition				Experiment			Literature	
J_i^{π} [a]	E_i (keV)	J_f^{π}	E_f (keV)	E_γ (keV)	I	I^{rel}	I [b]	I^{rel} [c]
(?)	2810.4(6)[q]	4^+	404.18	2406.2(7)[o]	0.38(11)	100(29)		
		6^+	770.40	2039.9(10)[o,p]	0.11(4)	29(11)		
(?)	2818.4(2)	4^+	404.18	2414.2(2)[o]	1.60(18)	100(11)		
		6^+	770.40	2048.0(2)[o]	0.19(6)	12(4)		
		2^+	828.66	[1990]	<0.07	<4	0.21(9)	11(5)
		3^+	1022.10	[1796]	<0.13	<8	0.46(4)	25.0(22)
		4^+	1088.28	1730.1(2)	0.57(6)	36(4)	0.49(9)	27(5)
		4^+	1168.4	1649.7(2)	1.37(11)	86(7)	1.84(4)	100.0(22)
				[1525][v]			0.68(7)	37(4)
		5^+	1335.51	1482.7(2)[o]	0.30(5)	19(3)		
		3^-	1368.53	1450.0(8)[o,p]	0.15(6)	9(4)		
		6^+	1437.28	1380.9(2)[o]	0.65(6)	41(4)		
		6^+	1525.3	1293.4(15)[o]	0.27(4)	17(3)		
		(5^-)	1526.0	1292.3(3)[o]	0.87(11)	54(7)		
		$(4)^+$	1627.5	1191.1(5)	0.43(6)	27(4)	0.20(7)	11(4)
		(?)	1857.82	960.6(3)[o]	0.69(7)	43(4)		
		(6)	1898.5	919.7(15)[o]	0.13(5)	8(3)		
		(?)	1933.6	884.3(8)[o]	0.11(5)	7(3)		
(?)	2823.3(2)[dd]	4^+	404.18	2419.2(2)	3.3(3)	100(9)	2.93(6)	100.0(20)
		6^+	770.40	2052.8(2)[o]	0.69(11)	21(3)		
		2^+	828.66	[1994]	<0.07	<2	0.13(9)	4(3)
		2^+	890.50	[1932]	<0.11	<3	0.26(4)	8.9(14)
		4^+	1168.4	1654.0(11)[o,p]	0.14(6)	4.2(18)		
		(5^-)	1526.0	1297.3(2)[o]	0.33(8)	10(2)		
		(?)	1857.82	965.3(8)[o]	0.10(5)	3.0(15)		
(?)	2833.6(4)[q]	4^+	404.18	2429.5(7)[o]	0.63(9)	100(14)		
		6^+	770.40	2063.2(4)[o]	0.23(4)	37(6)		
(?)	2894.9(4)[q]	4^+	404.18	2490.7(6)[o]	0.21(7)	100(33)		
		2^+	890.50	2004.2(9)[o,p]	0.10(4)	48(19)		
		3^+	1022.10	1872.9(4)[o]	0.21(5)	100(24)		
(?)	2981.5(13)[q]	4^+	404.18	2577.3(13)[o]	0.33(7)	100(21)		

[a]Level spin assignments are nominal assignments from the evaluation [13], except as noted.

[b]Literature values for absolute intensities are from the evaluated ^{156}Ho EC decay data of Ref. [13], which were based primarily upon Ref. [22], except as noted.

[c]Literature values for relative intensities are from the adopted γ radiations of the evaluation [13], except as noted. Where the evaluation [13] gave more than one possible adopted value, all are listed here.

[d]The literature γ-ray intensity is deduced from conversion electron data only, using an assumed conversion coefficient from Ref. [22].

[e]Listed in the evaluation [13] as 5.9, but the intensity and conversion coefficient given in the original literature [22] actually yielded 1.9.

[f]Listed in the evaluation [13] as 7.2, but the intensity and conversion coefficient given in the original literature [22] actually yielded 3.5. The evaluation also notes larger but ambiguous intensities reported in $(\alpha,4n)$ [20].

[g]Transition was previously reported, but not in β decay.

[h]Relative intensity from $(\alpha,4n)$ was listed in the evaluation [13] as 57, but the intensities given in the original literature [20] actually yielded 45(14). The uncertainties from the original $(p,4n)$ literature [21] are used here to obtain the value 11(2).

[i]Relative intensity from $(\alpha,4n)$ was listed in the evaluation [13] as 370, but the intensities given in the original literature [20] actually yielded 557(90).

[j]Relative intensity from $(\alpha,4n)$ was listed in the evaluation [13] as 515. The uncertainties, and unrounded intensities, from the original literature [20] are used here to obtain 530(60).

[k]This is a literature I^{ce} value from conversion electron data from Ref. [22]. Reference [22] made no prediction for the corresponding γ-ray intensity since an unknown portion of the electron intensity may result from an $E0$ contribution.

[l]Level was previously reported, but not in β decay [13].

[m]Probable spin assignment for the identified level is given on the basis of observed transitions to levels of known spin.

TABLE I. *(Continued.)*

[n]The level at 1382.3(2) keV may be identified with the adopted (3^-) level at 1385(5) keV [13] reported in (p,t) scattering [23].
[o]Gamma-ray line not previously reported, or not reported in this placement.
[p]Identification of the transition is tentative.
[q]Level not previously reported.
[r]Energy and intensity are deduced from gated spectrum after subtraction of contribution(s) from other placement(s). (Also see EPAPS tabulation [19].)
[s]Level is not identified as having been populated in β decay in the published literature [22] but is quoted as having been populated in an unpublished β-decay study [24].
[t]Transitions from the closely-spaced pair of levels at 1525.3(2) and 1526.0(2) keV are all potentially doublets. Each transition is assigned a primary placement as depopulating one of these levels on the basis of transition energy as measured in gated spectra but may contain a significant unresolved contribution depopulating the other member of the pair. (See the text.)
[u]The placement here, reported in $(\alpha,4n)$ [20], is noted by the evaluation [13] to be uncertain.
[v]A literature transition was reported to a level the existence of which is not supported by the present data. (See the text.)
[w]Limit obtained on any possible absolute intensity coincident with the alleged 1310-keV transition from Ref. [20], which is claimed as the only branch from the literature $(2^+)_{1447}$ level. (See the text.)
[x]The intensity for the adopted 178.93(20) keV branch is omitted in the evaluation [13], with an indication that the placement of the transition in the level scheme is uncertain. The relative intensity for this branch deduced from the original literature [20] is 133(43).
[y]Peak in the gated spectrum has an abnormally large width.
[z]The evaluation [13] did not deduce relative intensities for the 1039- and 594-keV branches. The 1039-keV branch was reported in (HI,xn), $(\alpha,4n)$, and $(p,4n)$ [25,20,21]. The 594-keV branch was only reported in $(\alpha,4n)$ and $(p,4n)$ [20], and the line was noted by the authors to contain ^{127}I contamination.
[aa]The nominal spin assignment for the adopted level at 1898.64(10) keV [13] is $(6,7^-)$. (See the text.)
[bb]The level at 2408.7(4) keV may be identified with the adopted (2^-) level at 2409.64(20) keV [13] reported in β decay [22]. (See the text.)
[cc]The level at 2516.6(7) keV may be identified with the adopted $(1)^-$ level at 2517.55(16) keV [13] reported in β decay [22]. (See the text.)
[dd]The level at 2823.3(2) keV may be identified with the adopted level at 2822.2(4) keV [13] reported in β decay [22].

III. EXPERIMENTAL RESULTS

A. Overview of results

The coincidence data from the present experiment provided placement and intensity information on over 250 γ-ray transitions in ^{156}Dy. The γ-ray transition energies, placements, and absolute and relative intensities deduced in this experiment are summarized in Table I. Supplementary information, including observed coincidence relations and data on unplaced transitions, is available through the Electronic Physics Auxiliary Publication Service (EPAPS) [19]. The level scheme constitutes a substantial revision to that found in the literature [13]: over 50 new levels are identified, numerous levels previously claimed from β-decay data are

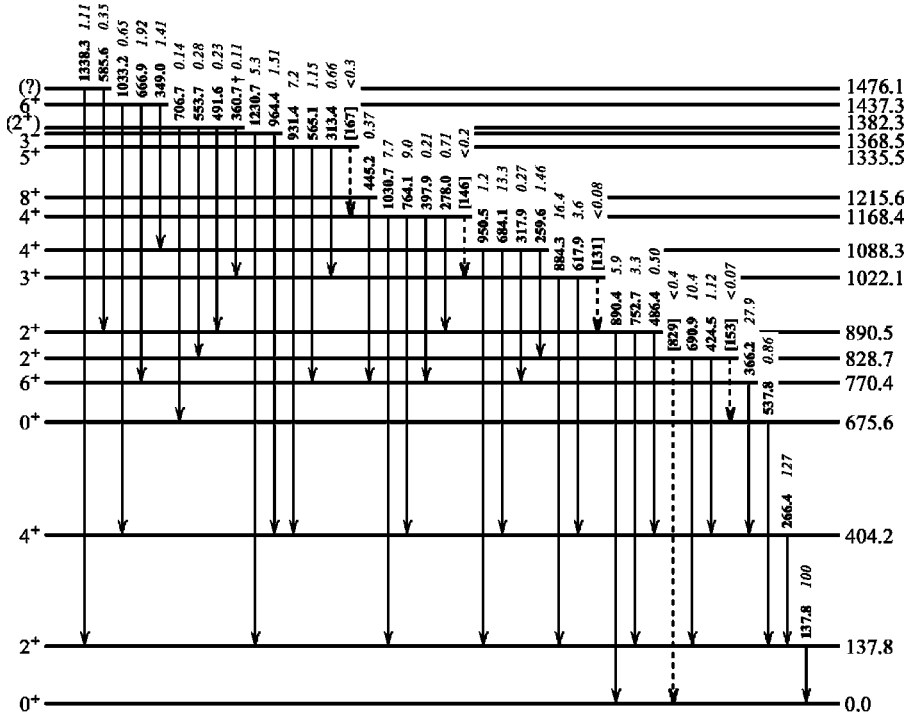

FIG. 4. Low-lying levels in ^{156}Dy populated in ^{156g}Ho β decay and their depopulating γ-ray transitions (with energies and intensities from Table I). Unobserved transitions for which intensity limits are obtained contradicting previously reported values are indicated by dashed arrows. Tentative placements are marked with a dagger (†).

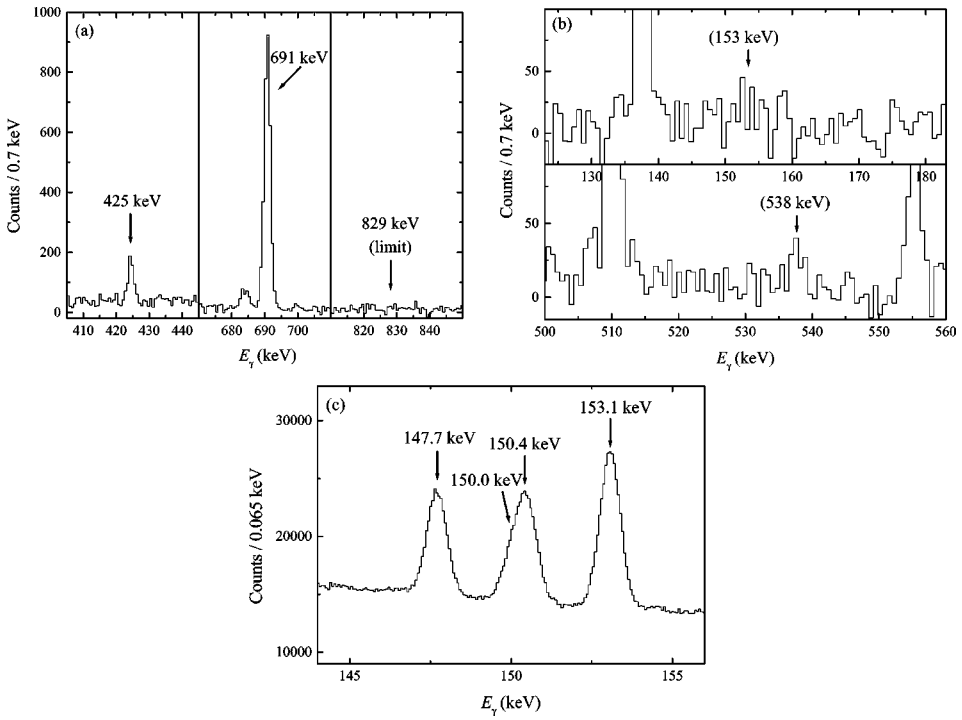

FIG. 5. Transitions from the 2^+ level at 829 keV. (a) Composite spectrum gated on 260-, 796-, 1416-, and 1479-keV transitions feeding the 2^+_{829} level, showing the 424-, 691-, and unobserved 829-keV branches from this level. (b) Spectra gated on the 538-keV $0^+_{676}\rightarrow 2^+_{138}$ transition (top) and on the expected energy of the 153-keV $2^+_{829}\rightarrow 0^+_{676}$ transition (bottom), which allow a limit to be placed upon coincidences between these transitions. (c) LEPS detector singles spectrum showing the strong contaminant peaks at 147.7 keV (^{157}Dy), 150.0 keV (^{157}Ho), 150.4 keV (^{157}Dy), and 153.1 keV (^{157}Dy).

found to be unsubstantiated, and the decay properties of many of the remaining levels are substantially modified. The level scheme for levels populated below 1500 keV is shown in Fig. 4.

B. Transitions depopulating low-lying levels

We discuss now the experimental results for levels which are of current interest in the structural interpretation of ^{156}Dy, elaborating upon the basic information presented in Table I. For simplicity, the notation $J^\pi_{E_{\rm ex}\,({\rm keV})}$ will be used to denote the level of spin assignment J^π at excitation energy $E_{\rm ex}$. (Spin assignments are taken from Ref. [13] unless information affecting the spin assignment has been obtained from the present experiment.) Relative intensities quoted in the following discussion are normalized to $I^{\rm rel}=100$ for the strongest branch from each level (see Table I).

2^+_{829}: Measurement of the branching properties of this level provided much of the initial motivation for the present experiment, as this level is central to interpretation of the low-lying collective structure of ^{156}Dy and considerable ambiguities existed in the literature (Table I). The relative intensities of the two strongest branches from this level, to the 2^+ and 4^+ members of the yrast band, were confirmed. However, the 829-keV transition to the ground state is highly suppressed, in spite of its having a larger transition energy than the other branches. Only a limit on its intensity could be obtained, $I^{\rm rel}_{829}<4$, from spectra gated on transitions feeding 2^+_{829} [Fig. 5(a)]. Previously an intensity $I^{\rm rel}_{829}=16(18)$ was proposed from an $(\alpha,4n)$ study [20].

Wildly discrepant intensities for the 153-keV $2^+_{829}\rightarrow 0^+_{676}$ transition have been reported. Much of the confusion probably results from the presence of a strong 153.0-keV transi-

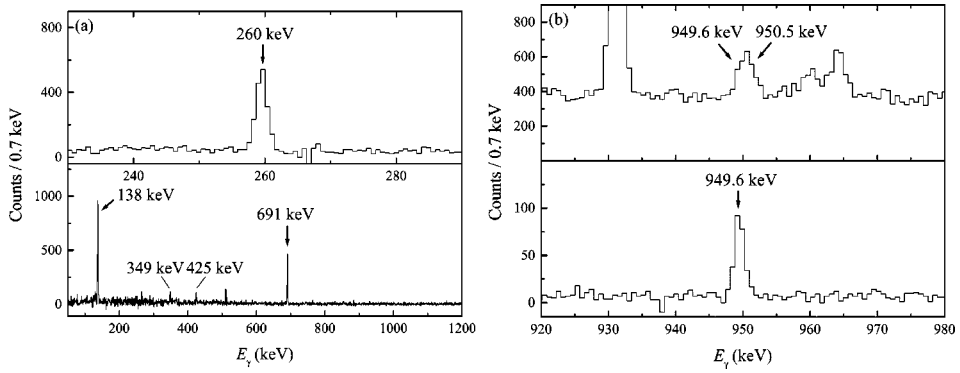

FIG. 6. Transitions from the 4^+ level at 1088 keV. (a) Spectra gated on the 691-keV $2^+_{829}\rightarrow 2^+_{138}$ (top) and 260-keV $4^+_{1088}\rightarrow 2^+_{829}$ (bottom) transitions, supporting the placement of the 260-keV transition and allowing measurement of its intensity. (b) Spectra gated on the 138-keV $2^+_{138}\rightarrow 0^+_0$ (top) and 890-keV $2^+_{890}\rightarrow 0^+_0$ (bottom) transitions, illustrating the 950.5-keV branch from the 4^+_{1088} level and the doublet 949.6-keV $(?)_{1840}\rightarrow 2^+_{890}$ transition.

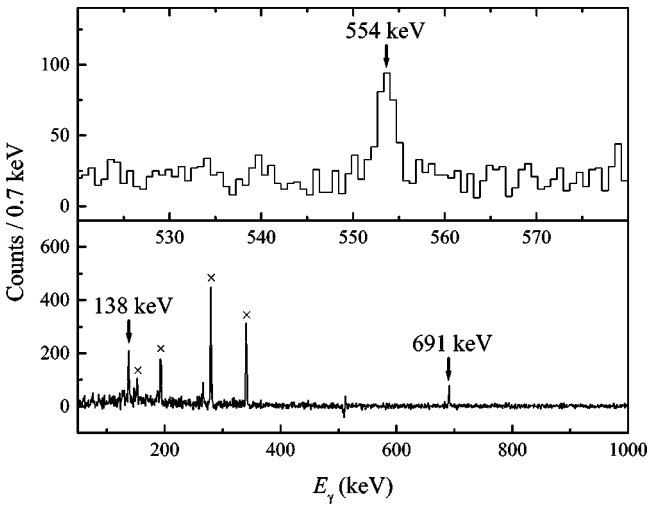

FIG. 7. Gated coincidence spectra providing evidence of the placement of the 554-keV transition as a branch from the $(2^+)_{1382}$ level to the 2^+_{829} level. (a) Spectra gated on the 691-keV $2^+_{829} \rightarrow 2^+_{138}$ (top) and 554-keV (bottom) transitions. Contaminant transitions coincident with the 555-keV transition in ^{157}Dy are indicated with a cross ($\times$).

tion in ^{157}Dy—relative intensities as large as $I^{\rm rel}_{153} \approx 144$ were found in experiments subject to ^{157}Dy contamination [20,21]. The prior β-decay work [22] estimated $I^{\rm rel}_{153} \approx 1.9$ from conversion electron singles data. In singles, the γ-ray spectrum at this energy in the present experiment is overwhelmingly dominated by the contaminant transition in ^{157}Dy [Fig. 5(c)]. Coincidences with the 538 keV $0^+_{676} \rightarrow 2^+_{138}$ transition were not observed [Fig. 5(b)], allowing a limit of $I^{\rm rel} < 0.7$ to be placed on the intensity of the $2^+_{829} \rightarrow 0^+_{676}$ transition, which eliminates the various previously claimed intensities for this transition.

2^+_{890}: The reported intensities for the transitions to the yrast 0^+, 2^+, and 4^+ states are essentially confirmed, with some reduction in uncertainty for the intensity of the 486 keV $2^+_{890} \rightarrow 4^+_{404}$ transition. A weak ($\sim$5%) doublet contribution is found in the 890-keV $2^+_{890} \rightarrow 0^+_0$ transition. Limits are placed upon any possible transitions to the 0^+_{676} and 2^+_{829} states. (A $2^+_{890} \rightarrow 2^+_{829}$ γ-ray transition is deduced in Ref. [22] on the basis of conversion electron data, but at a level marginally below the sensitivity of the present limit.)

4^+_{1088}: The most important result obtained for this level is the confirmation of the existence of the ''in-band'' 260-keV $4^+_{1088} \rightarrow 2^+_{829}$ transition, together with a reliable intensity measurement [$I^{\rm rel}_{260} = 11.0(10)$]. Coincidences between this transition and transitions depopulating the 2^+_{829} level or feeding the 4^+_{1088} level are shown in Fig. 6(a). (Prior values for the relative intensity had ranged from about 11 to 45 [20,21], with nonobservation in β decay [22].)

The intensities of the transitions from the 4^+_{1088} state to the yrast band members are also different from those previously reported. The 950-keV $4^+_{1088} \rightarrow 2^+_{138}$ transitions is found to contain a $(?)_{1840} \rightarrow 2^+_{890}$ doublet contribution ($\sim$37% of the total intensity) [Table I and Fig. 6(b)], and the uncertainty in the intensity of the 318-keV $4^+_{1088} \rightarrow 6^+_{770}$ transition is considerably reduced.

4^+_{1168}: The strong 1031- and 764-keV branches to the yrast 2^+ and 4^+ states are essentially unchanged from Ref. [22], although the 1031-keV transition is found to have a weak ($\sim$1.4%) doublet contribution. The 398-keV $4^+_{1168} \rightarrow 6^+_{770}$ branch is now clearly identified [$I^{\rm rel}_{398} = 2.3(6)$] from coincidences. (Previous claims for the intensity of this transition had disagreed radically, with nonobservation in β decay [22].) The intensity measured for the ''in-band'' 278-keV $4^+_{1168} \rightarrow 2^+_{890}$ branch is modified ($\sim$37% decrease) relative to the value from Ref. [22]. A limit placed on the possible 146-keV branch to the 3^+_{1022} level ($I^{\rm rel}_{146} < 3$) excludes an extremely large relative intensity ($\sim$530) reported in (α,4n) [20], which perhaps resulted from contamination by the 147.7 keV transition in ^{157}Dy [Fig. 5(c)]. (A weaker γ-ray transition deduced from conversion electron data [22] is not excluded by the present limit.)

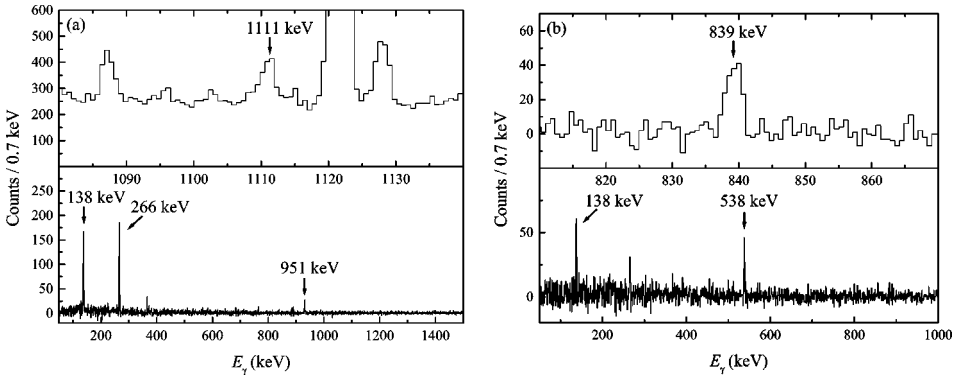

FIG. 8. Gated coincidence spectra providing evidence for branching transitions from the identified level at 1515 keV to 4^+ and 0^+ levels, suggesting a (2^+) spin assignment. (a) Spectra gated on the 266-keV $4^+_{404} \rightarrow 2^+_{138}$ transition (top) and the 1111.2-keV $(2^+)_{1515} \rightarrow 4^+_{404}$ transition (bottom), supporting the placement of the latter transition. The 1111-keV peak in the top spectrum is a doublet, containing a contribution from the 1110.7-keV $(?)_{2445} \rightarrow 5^+_{1336}$ transition, which also produces the coincidence with the 951 keV $5^+_{1336} \rightarrow 4^+_{404}$ transition observed in the bottom spectrum. (b) Spectra gated on the 538-keV $0^+_{676} \rightarrow 2^+_{128}$ transition (top) and the 839-keV $(2^+)_{1515} \rightarrow 0^+_{676}$ transition (bottom), supporting the placement of the latter transition.

$(2^+)_{1382}$: A weakly-populated level is identified at 1382.3(2) keV on the basis of γ-ray branches to the 0^+_{676}, 2^+_{829}, 2^+_{890}, and possibly 3^+_{1022} levels deduced from coincidences with the transitions depopulating these respective levels (Fig. 7 and EPAPS [19]). The present level may be identified with the (3^-) level at 1385(5) keV [13], previously only reported in the (p,t) reaction [23], for which no prior γ-ray information was known. Observation of the γ-ray branch to an excited 0^+ state, together with the tentative transition to a 3^+ state, suggests a (2^+) spin assignment instead, although a spin of 3^- cannot be excluded if the transition to the 0^+_{676} state is taken to be of $E3$ multipolarity.

6^+_{1437}: The intensities found for the strong 667- and 349-keV branches to the 6^+_{770} and 4^+_{1088} levels are in agreement with the literature. However, the intensity of the 1033-keV $6^+_{1437}\rightarrow 4^+_{404}$ transition, which was previously not observed in β decay, is found to have about twice the value obtained from $(\alpha,4n)$ [20].

$(2^+)_{1515}$: A level at 1515.0(2) keV is identified on the basis of transitions to the 4^+_{404}, 0^+_{676}, and 2^+_{890} states. These transitions suggest a 2^+ spin assigment (Fig. 8), although a spin of 3^- cannot be excluded if $E3$ multipolarity is considered.

6^+_{1525} and $(5^-)_{1526}$: A closely spaced pair of levels lies at 1525.3(2) and 1526.0(2) keV. All transitions feeding or depopulating these levels are potentially doublets at a $\sim$0.7-keV separation, and division of the intensities has been a challenge to all studies of these levels [20,21]. (In fact, the prior published β-decay work [22] failed to identify the lower of the two levels, but unpublished β-decay work [24] cited in Ref. [20] did observe both levels.) At least one of these levels decays to each of the levels 4^+_{404}, 6^+_{770}, 4^+_{1088}, and 4^+_{1168}. [The 190-keV branch to the 5^+_{1336} level reported in $(\alpha,4n)$ [20] is excluded by the present data.] The present data are likewise not unambiguous about the assignment of intensities. However, the centroid energies of the observed peaks in gated spectra suggest that most of the intensity in the 755-keV transition to the 6^+_{770} level and in the 356 keV transition to the 4^+_{1168} level is depopulating the 6^+_{1525} level, while most of the observed intensity in the 1122-keV transition to the 4^+_{404} level and in the 438-keV transition to the 4^+_{1088} level is depopulating the $(5^-)_{1526}$ level. (Estimated limits on the intensity in the other portion of each potential doublet are given in Table I.) Note that the adopted spin assignments [13] of the two levels, which are based upon measured conversion coefficients for the depopulating transitions, are rather speculative given the uncertainties in γ-ray intensities.

Among the higher-lying levels, several previously reported in β decay [22] are observed—$(3)^-_{1609}$, $(4)^+_{1627}$, 2^+_{2090}, 4^+_{2307}, $(?)_{2409}$ [previously (2^-)], $(?)_{2517}$ [previously $(1)^-$], $(?)_{2818}$, and $(?)_{2823}$—albeit some with significantly modified decay properties. Three levels previously only identified in in-beam studies [20,21,25]—7^+_{1729}, 7^-_{1810}, and $(6)_{1898}$ [previously $(6,7^-)$]—are also observed, yielding new information of their branching properties. We comment here only on a few of the confirmed higher-lying levels, those for which the new data modify the spin assignment. (Details on all are given in Table I.)

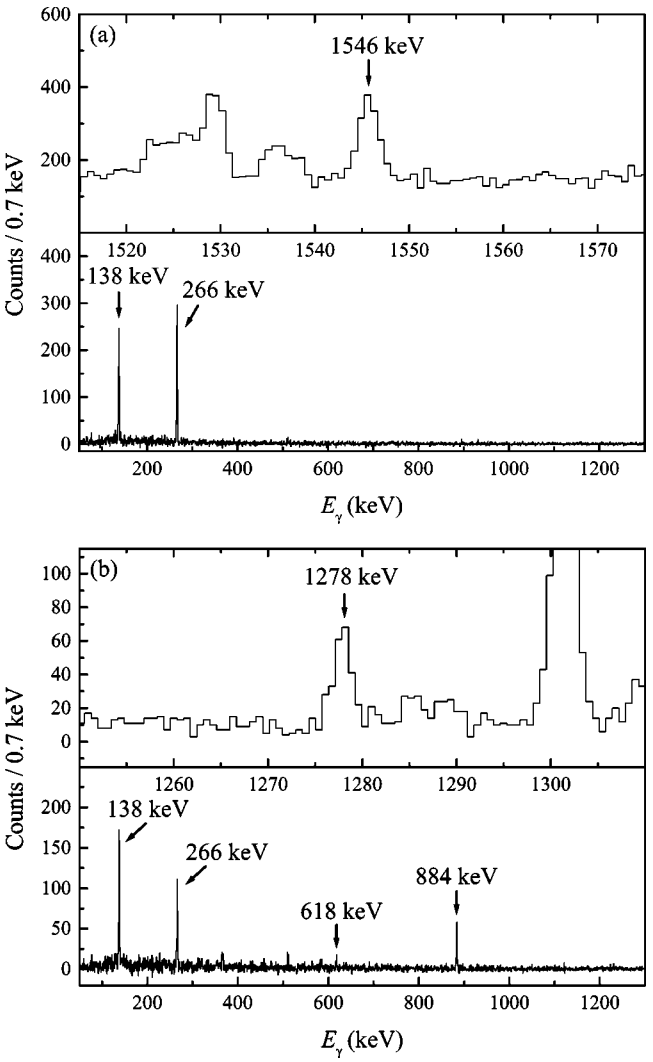

FIG. 9. Gated coincidence spectra providing evidence for the existence of levels at 1950 and 2300 keV. (a) Spectra gated on the 266-keV $4^+_{404}\rightarrow 2^+_{128}$ transition (top) and the 1546 keV $(?)_{1950}\rightarrow 4^+_{404}$ transition (bottom). (b) Spectra gated on the 884-keV $3^+_{1022}\rightarrow 2^+_{138}$ transition (top) and the 1278-keV $(?)_{2300}\rightarrow 3^+_{1022}$ transition (bottom), supporting its placement as directly feeding the 3^+_{1022} level.

$(6)_{1898}$: The adopted level at 1898.64(10) keV [13] had been assigned a spin of $(6,7^-)$ based upon results from $(\alpha,4n)$, $(p,4n)$, and (HI,xn) studies [20,25]. The present data show a transition to a 5^+ level, which eliminates the possible 7^- assignment.

$(?)_{2409}$: The adopted level at 2409.64(20) keV [13] had been assigned a spin of (2^-), based upon a supposed 880-keV $M1$ γ-ray transition to a (1^-) level at 1529 keV and the presence of γ-ray transitions to 4^+ levels. This spin assignment would have required both transitions to 4^+ levels to be $E3$ in character, constituting a fairly unusual situation. However, the present data show that there is no evidence for the (1^-) level at 1529 keV (see Sec. III C) or for the 880-keV branch to this level. Several new branches from the $(?)_{2409}$

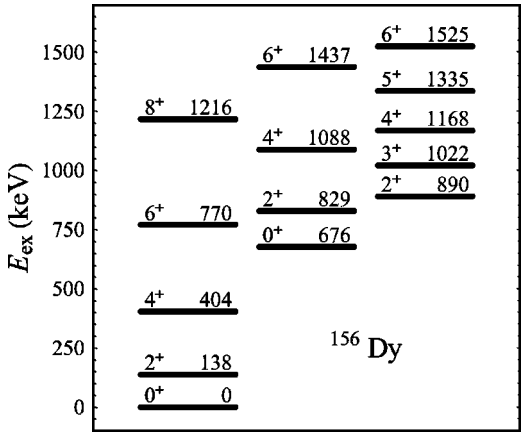

FIG. 10. Low-lying level scheme of ^{156}Dy, showing members of the first three positive-parity bands, following the band assignments of Ref. [13].

level are observed, and all branches to levels of known spin are to 2^+, $3^\pm$, or 4^+ levels.

$(?)_{2517}$: The present level at 2516.6(7) keV may be identified with the adopted level at 2517.55(16) keV [13], which had a spin assignment of (1^-) based upon a supposed $E2$ γ-ray transition to a $(3)^-$ level and a γ-ray transition to a 0^+ level. (There is an observed transition to a 4^+ level, which this assignment would have required to be $E3$ in nature.) However, the present data eliminate the claimed 907-keV transition to the $(3)^-_{1609}$ level and the 1841-keV transition to the 0^+_{676} level. This leaves only transitions to 2^+, 3^+, and 4^+ levels, and possibly a transition to a 3^- level (Table I). It also should be noted that the level energy calculated from the transition energy of the 1493.8(10) keV branch from this level (as measured in a spectrum gated on the 884-keV transition) disagrees with that calculated from the transition energy of the 1348.9(5) keV branch (as measured in spectra gated on the 764- and 1031-keV transitions) and from the other two tentatively placed branches. Even though the discrepancy ($\sim$1.4 keV) is within the extreme range of the energy uncertainties, it calls into question the identity of the level as a single level.

Several new levels are identified as well (Table I). Many of the new levels are identified on the basis of several corroborating branching or feeding transitions, each independently placed from coincidence data. Other levels are identified on the basis of only one or two branches. These have been retained in the tabulation when there is fairly strong evidence for their placement from coincidence relations (see Fig. 9). [Some of the ''new'' levels below 2250 keV likely correspond to levels previously reported in (d,d') or (p,t) studies [23,26], but the low energy resolution of such studies precludes the establishment of an unambiguous correspondence.]

C. Previously reported levels from β decay for which no evidence is found

The prior β-decay study [22] of ^{156}Dy identified levels on the basis primarily of singles γ-ray data, together with singles conversion electron data and some very limited coincidence data. Identification of levels from a singles spectrum relies upon the recognition of groups of γ-ray lines satisfying Ritz sum energy combinations. This process is extremely challenging for ^{156}Dy due to the large number of levels populated and consequently high line density in the spectrum: for a large number of lines many accidental energy combinations can exist within the experimental energy resolution, and the complicated nature of the spectrum hinders the accurate identification of lines and determination of their energies for use in the Ritz procedure in the first place. The availability of high-statistics γ-ray coincidence data, as in the present study, provides at least two benefits: placement information from coincidence relations and more reliable energy determinations from clean gated spectra.

Since a large number of levels previously proposed on the basis of β decay are found to be unsubstantiated by the present data, it is worth summarizing the evidence used in dismissing these levels. Each such level was invoked to explain several γ rays observed in singles. If substantially all of the intensity for a γ ray is now accounted for by one or more new placements from coincidence information, the need for the original proposed placement is obviated. The suggested

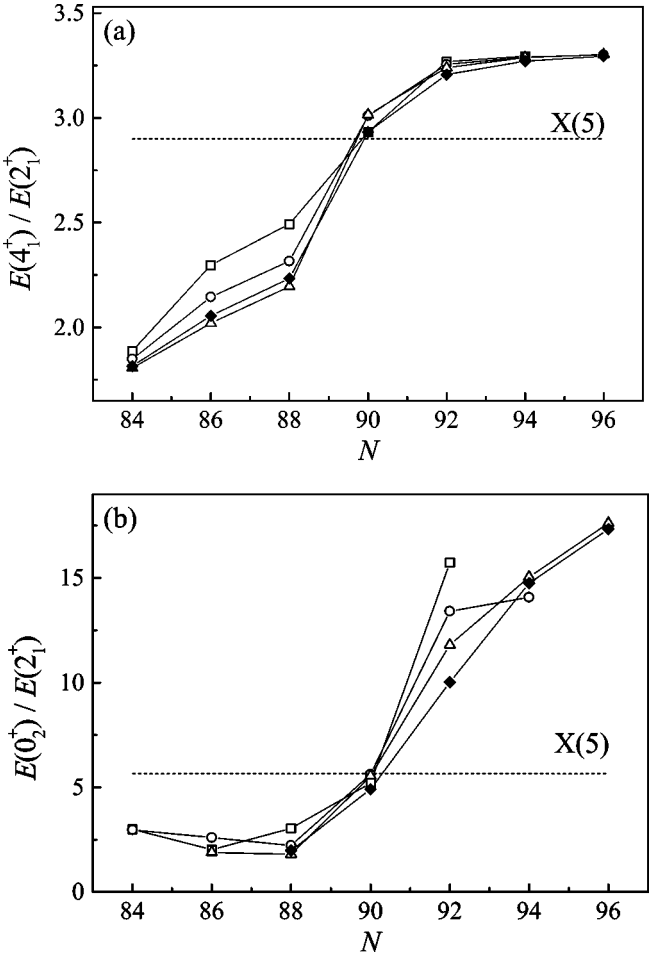

FIG. 11. Evolution of the (a) 4^+_1 and (b) 0^+_2 energies (normalized to the 2^+_1 energy) across the $N=90$ transition region, for the Nd (□), Sm (○), Gd (△), and Dy (♦) isotopic chains, compared with the $X(5)$ prediction.

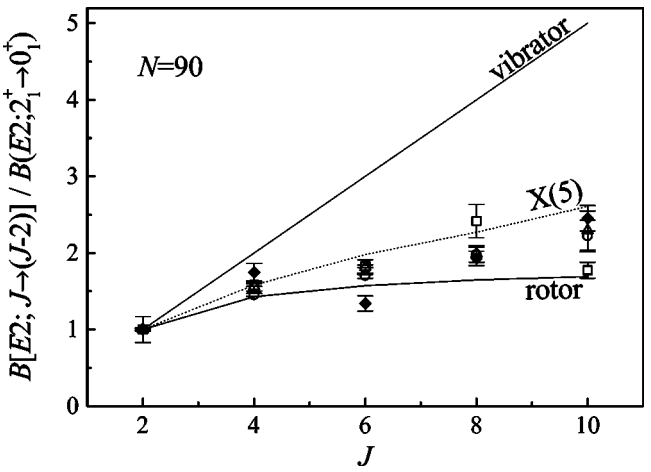

FIG. 12. Yrast band $B(E2)$ values, normalized to the $2_g^+ \rightarrow 0_g^+$ transition, for the $N=90$ isotones ^{150}Nd (□), ^{152}Sm (○), ^{154}Gd (△), and ^{156}Dy (♦). The rotor, $X(5)$, and vibrator predictions are shown for comparison. Experimental values are from Refs. [11,13,18,34,35]. (Figure from Ref. [12].)

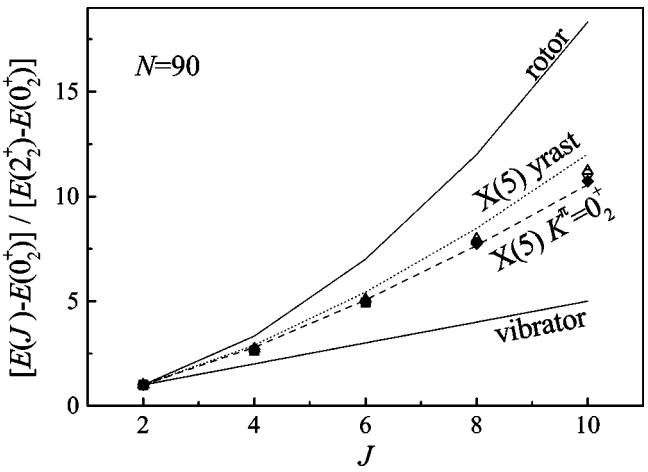

FIG. 13. $K^\pi = 0_2^+$ band level energies (taken relative to the band head and normalized to the 2^+ band member), for the $N=90$ isotones ^{150}Nd (□), ^{152}Sm (○), ^{154}Gd (△), and ^{156}Dy (♦). The $X(5)$ predictions both for this band (dashed line) and for the yrast band $[E(J)/E(2_1^+)]$ (dotted line) are shown, illustrating the differing spin dependences discussed in the text. The rotor and vibrator predictions are also indicated.

placements also imply coincidences involving the γ rays, and a quantitative limit can be placed on such coincidences from the present data. Detailed discussions of a few of the most important low-lying dismissed levels follow.

$(1,2^+)_{1219}$: This level was proposed in β decay [22] to explain six γ-ray transitions, placed as two branches and four feeding transitions. The prior study identifies a 1218.9(4)-keV line of intensity 0.74(11), which it places as a branch to the ground state. The present coincidence data show this intensity to be accounted for (within uncertainties) by two new transitions: a 1217.2(3)-keV $(?)_{2386} \rightarrow 4^+_{1168}$ transition of intensity 0.25(7) and a 1218.9(5)-keV $4^+_{2307} \rightarrow 4^+_{1088}$ transition of intensity 0.39(10). Ref. [22] also reports a 1081.38(20)-keV line of intensity 1.01(6), which it places as a branch to 2^+_{138}, supported by an observed qualitative coincidence with the $2^+_{138} \rightarrow 0^+_0$ transition. The present coincidence data show there to be a 1081.18(9) keV $(?)_{2103} \rightarrow 3^+_{1022}$ transition of intensity 0.64(5). This leaves a residual intensity of 0.4(2) feeding the 2^+_{138} level in this energy region, observed in a spectrum gated on the 138-keV transition after subtraction of the known placement. The two stronger supposed feeding transitions, a 582.6(4)-keV transition of intensity 0.24(4) and a 2428.0(5)-keV transition of intensity 0.35(4), are noncoincident with the depopulating transitions at a level inconsistent with the prior decay scheme. (From the present data, the coincident intensity of any possible 583-keV transition with a 1081-keV transition is found to be <0.08, and that with a 1219 keV transition is <0.05. The coincident intensity of any 2428-keV transition with a 1081-keV transition is <0.06, and that with a 1219-keV transition is <0.07.) The 2428-keV γ-ray line is now replaced by a 2429.5(7)-keV $(?)_{2833} \rightarrow 4^+_{404}$ transition of intensity 0.63(9).

1^-_{1293}: This level was identified in β decay [22] on the basis of two depopulating transitions and five feeding transitions. (A discrepancy of ~0.67 keV existed, however, between the level energies deduced from the two different depopulating transitions.) Reference [22] reported a 1292.85(22)-keV transition of intensity 1.28(6), which it gave a $1^-_{1293} \rightarrow 0^+_0$ placement. However, this singles intensity is now fully accounted for by three transitions (Table I)—a 1292.3(3)-keV $(?)_{2818} \rightarrow (5^-)_{1526}$ transition, a 1293.0(5)-keV $(?)_{2184} \rightarrow 2^+_{890}$ transition (tentative), and a 1293.4(15)-keV $(?)_{2818} \rightarrow 6^+_{1525}$ transition—with a combined intensity of 1.28(14). Most (~85%) of the singles intensity observed at this energy in the present experiment comes from a 1293.7(2)-keV contaminant transition from ^{116}Sn, most likely arising from ^{115}In neutron capture followed by ^{116m}In β decay to ^{116}Sn [27], identified by its coincidences with the 818-, 1097-, 1507-, and 1753-keV transitions in that nucleus. Reference [22] also reported a 1155.72(14) keV transition of intensity 2.14(5), qualitatively coincident with the $2^+_{138} \rightarrow 0^+_0$ transition, which it assigned a $1^-_{1293} \rightarrow 2^+_{138}$ placement.

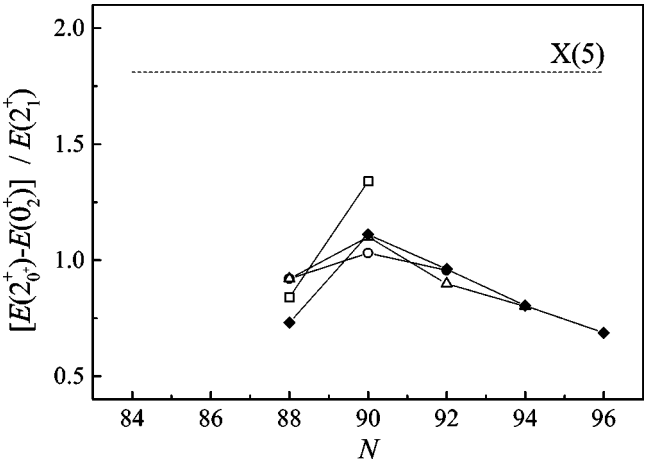

FIG. 14. Energy spacing scale of the excited 0^+ sequence relative to that of the yrast sequence, for the Nd (□), Sm (○), Gd (△), and Dy (♦) isotopic chains, compared with the $X(5)$ prediction.

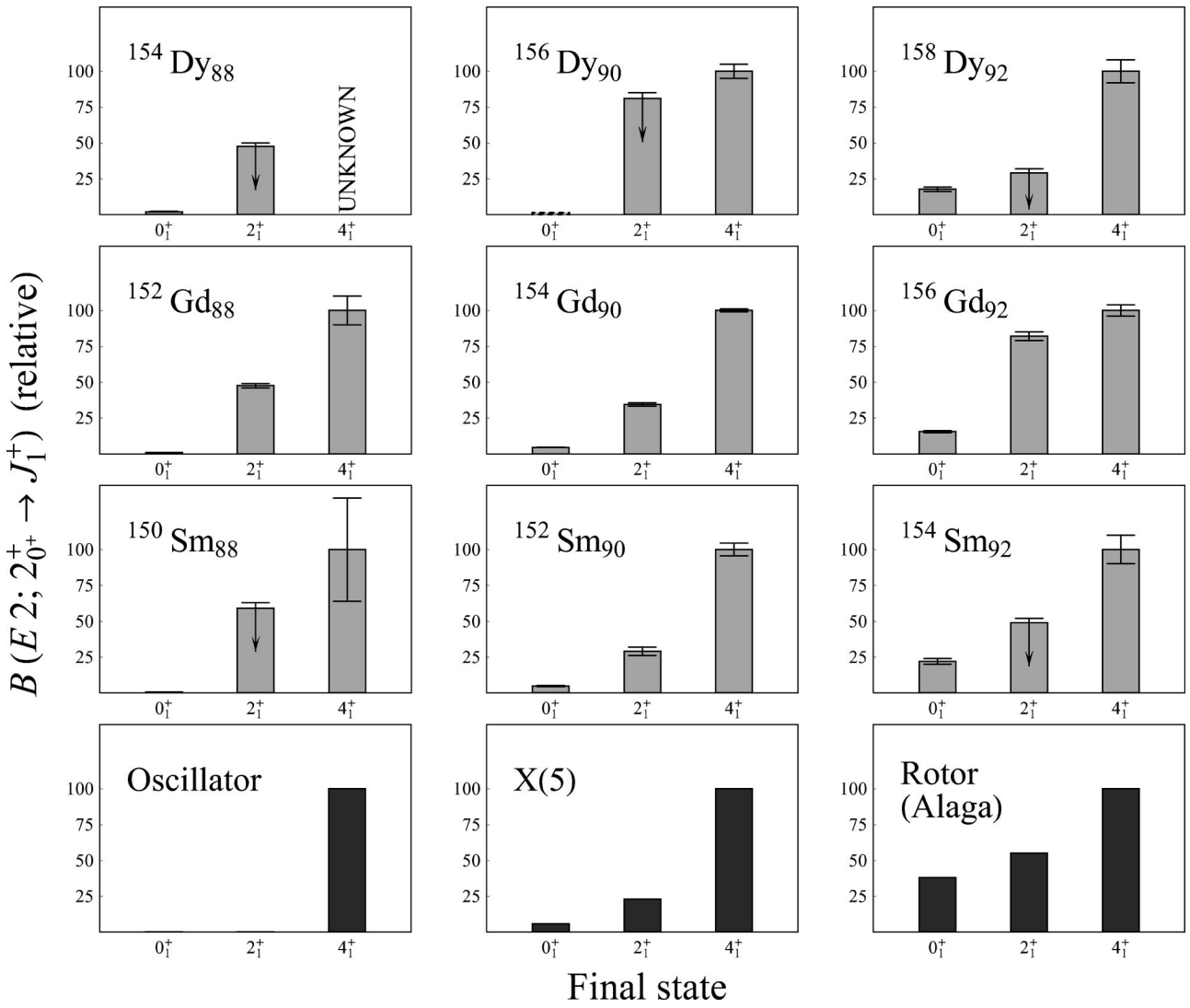

FIG. 15. Relative $B(E2)$ branching strengths for the ''interband'' transitions from the 2^+ state built upon the first excited 0^+ state to the yrast 0^+, 2^+, and 4^+ states, shown for the $N=88$, 90, and 92 isotopes of Dy, Gd, and Sm. The extreme harmonic oscillator limit, $X(5)$, and pure rotor limit predictions are provided for comparison at the bottom. Data are adopted values from Nuclear Data Sheets [13,18,34–36] except those for ^{152}Sm [8] and ^{156}Dy (present data). Error bars on the relative $B(E2)$ strengths include contributions from the experimental uncertainties in intensity and $E2/M1$ mixing ratios. [In the case of spin-unchanging transitions for which the $E2/M1$ mixing ratio is unknown, the $B(E2)$ strength is deduced assuming pure $E2$ multipolarity, and the possibility of arbitrarily large $M1$ contamination is indicated by a downward arrow.] Since the strength of the $2^+_2 \rightarrow 4^+_1$ transition in ^{154}Dy is unknown, the strengths of the $2^+_2 \rightarrow 0^+_1$ and $2^+_2 \rightarrow 2^+_1$ transitions are normalized (for comparison purposes) by setting the relative $2^+_2 \rightarrow 2^+_1$ strength equal to that in the neighboring isotone ^{152}Gd.

This intensity is now mostly accounted for by three transitions—an 1154.4(8)-keV $(?)_{2490} \rightarrow 5^+_{1336}$ transition (tentative), an 1155.3(2) $(?)_{2324} \rightarrow 4^+_{1168}$ transition, and an 1156.4 keV $(?)_{2245} \rightarrow 4^+_{1088}$ transition—with a combined intensity of 1.72(13). The intensities of all five feeding transitions are also accounted for (Table I), and all are found to be noncoincident with 1293- and 1156-keV transitions at intensity limits contradicting the earlier placements.

$(2^+)_{1447}$: This level was reported only in the $(a,4n)$ and $(p,4n)$ literature [20], but the placement given in that work was justified using information from an earlier unpublished β-decay study [24]. No evidence is found for the existence of this level in the present experiment.

2^+_{1518}: This level was identified in β decay [22] on the basis of two depopulating transitions and two feeding transitions. The reported singles intensities of these transitions are now accounted for by other placements (Table I and EPAPS [19]), and both feeding transitions are noncoincident with the depopulating transitions at intensity limits contradicting the earlier placements.

$(1^-)_{1529}$: This level was proposed in β decay [22] to explain seven γ-ray transitions, placed as two depopulating and five feeding transitions. The reported intensities of the 1529- and 1392-keV branching transitions and the 1274-, 1542-, and 1900-keV feeding transitions are now accounted for by other placements (Table I and EPAPS [19]), and all

feeding transitions are noncoincident with both depopulating transitions at intensity limits contradicting the earlier placements.

By similar arguments, there is no evidence for the existence of the levels claimed from β decay [22] at 1801, 1944, 2006, 2169, 2216, 2476, 2514, 2637, 2661, and 2803 keV, or above 2900-keV excitation energy.

IV. DISCUSSION OF THE LOW-LYING STRUCTURE

The structure of the low-lying levels of ^{156}Dy, summarized in Fig. 10, is most naturally approached in the context of its similarity to that of the neighboring $N=90$ isotones ^{150}Nd, ^{152}Sm, and ^{154}Gd, and so its observables will be discussed in comparison to those of the neighboring nuclei. The Nd, Sm, Gd, and Dy isotonic chains each undergo a rapid transition from spherical to axially symmetrically deformed structure (Fig. 11). As already alluded to, several basic observables (Figs. 1 and 11) indicate that all four isotopic chains reach essentially the same stage in the evolution of their structure at $N=90$. As early as the 1960s, studies of ^{152}Sm and ^{154}Gd highlighted the presence of unusual structural features in the $N=90$ nuclei. Experiments using (p,t) and (t,p) transfer reactions suggested the ''coexistence'' of well-deformed states with undeformed states in these nuclei [28–30], as later corroborated by the observation of unusually large electric monopole matrix elements [31]. These nuclei exhibit a form of band structure, but spectroscopic studies demonstrated that a conventional rotor picture with band mixing could not adequately account for the properties of the low-lying states in these nuclei [32]. More recent analysis using the interacting boson model (IBM) again suggests the coexistence of states with spherical and deformed structures within these nuclei, and the deduced potential energy surface is markedly flat in β (β-soft) [5]. Similar results are obtained in the geometric collective model (GCM) as well [33].

The essential features suggested for the structure of the $N=90$ nuclei—coexistence of states of different deformation in a β-soft potential—are incorporated into the $X(5)$ model [6], which has recently been proposed as a simple description of such transitional nuclei. This model is based upon the Bohr geometric Hamiltonian, specialized to a square well potential in β with an added term providing stabilization around $\gamma=0°$, and can be solved analytically for its eigenenergies and eigenfunctions in terms of the zeros of Bessel functions. The $X(5)$ model predicts a band structure resembling that of a rotor, but with substantially different energy ratios and $B(E2)$ strengths along the bands (Figs. 1 and 12). The model also predicts comparatively strong interband transitions, with branching properties differing from those of a true rotor.

The $X(5)$ predictions are especially straightforward to compare with experiment, since all predictions for energy ratios and $E2$ transition strength ratios involving the $K^\pi=0_1^+$ and $K^\pi=0_2^+$ bands are parameter independent. [The only free parameters affecting these bands are the mass parameter and square well width, which together serve only as scaling parameters controlling the overall energy scale and $B(E2)$ strength scale.] It was recently shown that the $X(5)$ model reproduces many of the important properties of ^{150}Nd [11] and ^{152}Sm [37].

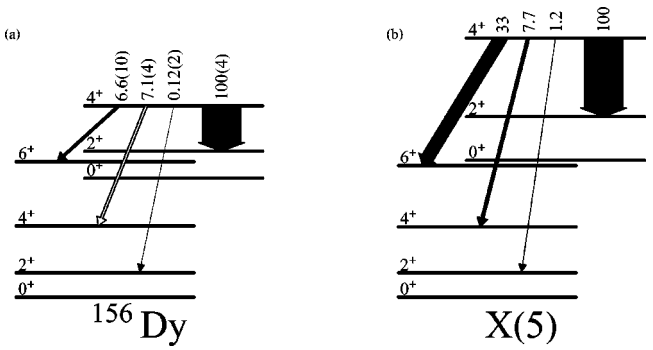

FIG. 16. Relative $B(E2)$ strengths for intraband and interband transitions from (a) the 4^+ member of the $K^\pi=0^+$ band in ^{156}Dy, together with (b) the $X(5)$ predictions. The open arrow for the spin-unchanging transition indicates the possibility of $M1$ contamination.

The energy spacing of the yrast band levels in ^{156}Dy closely matches the $X(5)$ predictions, as already noted (Fig. 1). The situation for the intraband $B(E2)$ strengths (Fig. 12) is less clear. The yrast band $B(E2)$ values were deduced from Coulomb excitation [38] and from recoil distance method lifetime measurements in (HI,xn) reactions [39,40]. The data generally indicate that the spin-dependence of the yrast band $B(E2)$ values is intermediate between the ideal vibrator and rotor limits, and the qualitative trend is consistent with the $X(5)$ predictions. The reported $B(E2)$ strength for the $6_g^+ \rightarrow 4_g^+$ transition, however, is anomalously low, substantially below even the rotor prediction. As there is some discrepancy in the data [39,40], and the 366 keV $6_g^+ \rightarrow 4_g^+$ transition was not well resolved in the ungated single-detector γ-ray spectra used by the existing studies (Fig. 1 of Ref. [39]), a remeasurement making use of gated coincidence techniques (e.g., the differential decay curve method [41]) could provide valuable clarification.

In the $X(5)$ model, the successive $K^\pi=0^+$ bands differ from each other in both the energy ratios and energy spacing scale of levels within the band. The level energy as a function of spin becomes successively more linear (oscillator-like) for more excited $K^\pi=0^+$ bands. This effect is clearly visible in the $X(5)$ predictions even for the first excited $K^\pi=0^+$ band (compare the dashed and dotted lines in Fig. 13). The spin dependence of the level energies for the $K^\pi=0_2^+$ band members in ^{156}Dy follows these predictions quite closely, as is also the case for the neighboring $N=90$ nuclei (Fig. 13). For the 2^+ and 4^+ band members specifically, this effect corresponds to a reduction in the ratio of 4^+ state energy to 2^+ state energy (taken relative to the band head) for the higher bands. In ^{156}Dy, the yrast band ratio $R_{4/2}(0_1^+) \equiv E(4_1^+)/E(2_1^+)$ is 2.93, while for the $K^\pi=0_2^+$ sequence the corresponding ratio $R_{4/2}(0_2^+) \equiv [E(4_2^+) - E(0_2^+)]/[E(2_2^+) - E(0_2^+)]$ is 2.70. The $X(5)$ predictions are 2.91 and 2.79 for the two bands, respectively.

The energy spacing *scale* for the $K^\pi=0_2^+$ band is predicted in $X(5)$ to be much larger than for the yrast band, with

$[E(2_2^+)-E(0_2^+)]/E(2_1^+)\approx 1.81$. For the Sm, Gd, and Dy isotopic chains, $N=90$ is the location of a local maximum (Fig. 14) in this ratio. However, the actual spacing is still much less than predicted by the $X(5)$ model. This serious discrepancy is encountered in descriptions of the $N=90$ nuclei using other collective models (the IBM and GCM) as well [8,33].

The intensity results for ^{156}Dy provide greatly improved information on relative $B(E2)$ strengths for transitions from the 2^+, 4^+, and 6^+ members of the first excited 0^+ band [absolute $B(E2)$ strengths are not available due to a lack of lifetime data], so it is now possible to make a meaningful comparison with the neighboring isotones and with model predictions. Figure 15 summarizes the branching properties for the 2^+ state in the first excited 0^+ sequence (denoted by $2_{0^+}^+$) for the $N=88$, 90, and 92 isotopes of Dy, Gd, and Sm. In going from $N=88$ to 92, the $2_{0^+}^+\rightarrow 0_1^+$ transition evolves from being highly suppressed relative to the $2_{0^+}^+\rightarrow 4_1^+$ transition [$B(E2;2_{0^+}^+\rightarrow 0_1^+)/B(E2;2_{0^+}^+\rightarrow 4_1^+)\approx 0.01$ at $N=88$] to having substantial strength [$B(E2;2_{0^+}^+\rightarrow 0_1^+)/B(E2;2_{0^+}^+\rightarrow 4_1^+)\approx 0.20$ at $N=92$]. The suppression for $N=88$ is reminiscent of the situation in the pure oscillator limit (in which case the 2^+ state directly above the 0_2^+ state is the 2_3^+ state), where the only one of the three transitions which is phonon-allowed is the $2_{0^+}^+\rightarrow 4_1^+$ transition (Fig. 15, bottom left panel), although clearly the $N=88$ nuclei are far from achieving pure oscillator structure. For the $N=92$ nuclei, the relative $B(E2)$ strengths begin to resemble the Alaga-rule strengths expected for a pure rotor (Fig. 15, bottom right panel), though the $N=92$ nuclei do notfully match these values. For the $N=90$ nuclei ^{152}Sm and ^{154}Gd (as well as ^{150}Nd [11], not shown) the agreement with the $X(5)$ predictions (Fig. 15, bottom center panel) is quite good. In ^{156}Dy, the $2_2^+\rightarrow 0_1^+$ transition is shown to be extremely weak. Its relative $B(E2)$ strength is at least a factor of 3–5 weaker than in the neighboring $N=90$ isotones or the $X(5)$ predictions. The $E2/M1$ mixing ratio for the spin-unchanging $2_2^+\rightarrow 2_1^+$ transition in ^{156}Dy is unknown, so only a limit can be placed on this transition's relative $B(E2)$ strength.

The relative strengths of the intraband and interband transitions from the 4^+ member of the $K^\pi=0_2^+$ band in ^{156}Dy, as deduced from the present revised intensities, are shown in Fig. 16(a). The strength scale of the interband transitions is much weaker relative to the intraband transitions than would be expected from the $X(5)$ predictions [Fig. 16(b)]. A similar weakness of the interband transitions relative to the $X(5)$ predictions is observed for the 2^+ and 4^+ members of the $K^\pi=0_2^+$ bands in ^{154}Gd and ^{152}Sm and 2^+ (but not 4^+) member in ^{150}Nd [8,11,18,35].

V. CONCLUSION

Extensive γ-ray coincidence spectroscopy has been carried out on the nucleus ^{156}Dy, populated in β^+/ε decay. Knowledge of the decay properties of the low-lying off-yrast levels has been greatly improved and new information has been obtained on the higher-lying level scheme, constituting a major revision relative to the previously published information. The new data allow direct comparison with the neighboring nuclei and with model predictions. This nucleus, like its isotones ^{150}Nd, ^{152}Sm, and ^{154}Gd, lies very near the critical point of the transition from spherical to axially-symmetric deformed shape and is well described by the $X(5)$ model.

ACKNOWLEDGMENTS

Valuable discussions with F. Iachello and P. von Brentano are gratefully acknowledged. This work was supported by the U.S. DOE under Grant Nos. DE-FG02-91ER-40609 and DE-FG02-88ER-40417, and by the German DFG under Grant No. Pi 393/1.

[1] R. F. Casten, N. V. Zamfir, and D. S. Brenner, Phys. Rev. Lett. **71**, 227 (1993).
[2] A. Wolf, R. F. Casten, N. V. Zamfir, and D. S. Brenner, Phys. Rev. C **49**, 802 (1994).
[3] J. N. Ginocchio and M. W. Kirson, Phys. Rev. Lett. **44**, 1744 (1980).
[4] A. E. L. Dieperink, O. Scholten, and F. Iachello, Phys. Rev. Lett. **44**, 1747 (1980).
[5] F. Iachello, N. V. Zamfir, and R. F. Casten, Phys. Rev. Lett. **81**, 1191 (1998).
[6] F. Iachello, Phys. Rev. Lett. **87**, 052502 (2001).
[7] R. F. Casten, M. Wilhelm, E. Radermacher, N. V. Zamfir, and P. von Brentano, Phys. Rev. C **57**, R1553 (1998).
[8] N. V. Zamfir, R. F. Casten, M. A. Caprio, C. W. Beausang, R. Krücken, J. R. Novak, J. R. Cooper, G. Cata-Danil, and C. J. Barton, Phys. Rev. C **60**, 054312 (1999).
[9] T. Klug, A. Dewald, V. Werner, P. von Brentano, and R. F. Casten, Phys. Lett. B **495**, 55 (2000).
[10] N. V. Zamfir, H. G. Börner, N. Pietralla, R. F. Casten, Z. Berant, C. J. Barton, C. W. Beausang, D. S. Brenner, M. A. Caprio, J. R. Cooper, A. A. Hecht, M. Krtička, R. Krücken, P. Mutti, J. R. Novak, and A. Wolf, Phys. Rev. C **65**, 067305 (2002).
[11] R. Krücken, B. Albanna, C. Bialik, R. F. Casten, J. R. Cooper, A. Dewald, N. V. Zamfir, C. J. Barton, C. W. Beausang, M. A. Caprio, A. A. Hecht, T. Klug, J. R. Novak, N. Pietralla, and P. von Brentano, Phys. Rev. Lett. **88**, 232501 (2002).
[12] M. A. Caprio, in *Mapping the Triangle*, edited by A. Aprahamian, J. A. Cizewski, S. Pittel, and N. V. Zamfir, AIP Conf. Proc. No. 638 (AIP, Melville, NY, 2002), p. 17.
[13] R. G. Helmer, Nucl. Data Sheets **49**, 383 (1986); **65**, 65 (1992).
[14] M. A. Caprio, N. V. Zamfir, R. F. Casten, C. J. Barton, C. W. Beausang, J. R. Cooper, A. A. Hecht, R. Krücken, H. Newman, J. R. Novak, N. Pietralla, A. Wolf, and K. E. Zyromski, Rom. J. Phys. **46**, 41 (2001).
[15] N. V. Zamfir and R. F. Casten, J. Res. Natl. Inst. Stand. Technol. **105**, 147 (2000).

[16] N. V. Zamfir, M. A. Caprio, R. F. Casten, C. J. Barton, C. W. Beausang, Z. Berant, D. S. Brenner, W. T. Chou, J. R. Cooper, A. A. Hecht, R. Krücken, H. Newman, J. R. Novak, N. Pietralla, A. Wolf, and K. E. Zyromski, Phys. Rev. C **65**, 044325 (2002).
[17] C. W. Beausang, C. J. Barton, M. A. Caprio, R. F. Casten, J. R. Cooper, R. Krücken, B. Liu, J. R. Novak, Z. Wang, M. Wilhelm, A. N. Wilson, N. V. Zamfir, and A. Zilges, Nucl. Instrum. Methods Phys. Res. A **452**, 431 (2000).
[18] A. Artna-Cohen, Nucl. Data Sheets **79**, 1 (1996).
[19] See EPAPS Document No. E-PRVCAN-66-014211 for additional tabular material. This document may be retrieved via the EPAPS home page (http://www.aip.org/pubservs/epaps.html) or by FTP (ftp://ftp.aip.org/epaps/).
[20] F. W. N. de Boer, P. Koldewijn, R. Beetz, J. L. Maarleveld, J. Konij, R. Janssens, and J. Vervier, Nucl. Phys. **A290**, 173 (1977).
[21] Y. El Masri, J. M. Ferté, R. Janssens, C. Michel, P. Monseu, J. Steyaert, and J. Vervier, Nucl. Phys. **A271**, 133 (1976).
[22] K. Y. Gromov, Z. T. Zhelev, K. Zuber, Y. Zuber, T. A. Islamov, V. V. Kuznetsov, H.-G. Ortlepp, and A. V. Potempa, Acta Phys. Pol. B **7**, 507 (1976).
[23] J. J. Kolata and M. Oothoudt, Phys. Rev. C **15**, 1947 (1977).
[24] P. Koldewijn, F. W. N. de Boer, B. J. Meijer, and J. Konijn (as quoted in Ref. [20]).
[25] M. A. Riley, J. Simpson, J. F. Sharpey-Schafer, J. R. Cresswell, H. W. Cranmer-Gordon, P. D. Forsyth, D. Howe, A. H. Nelson, P. J. Nolan, P. J. Smith, N. J. Ward, J. C. Lisle, E. Paul, and P. M. Walker, Nucl. Phys. **A486**, 456 (1988).
[26] T. Grotdal, K. Nybø, T. Thorsteinsen, and B. Elbek, Nucl. Phys. **A110**, 385 (1968).
[27] J. Blachot and G. Marguier, Nucl. Data Sheets **73**, 81 (1994).
[28] J. H. Bjerregaard, O. Hansen, O. Nathan, and S. Hinds, Nucl. Phys. **86**, 145 (1966).
[29] W. McLatchie, W. Darcey, and J. E. Kitching, Nucl. Phys. **A159**, 615 (1970).
[30] P. Debenham and N. M. Hintz, Nucl. Phys. **A195**, 385 (1972).
[31] J. L. Wood, E. F. Zganjar, C. de Coster, and K. Heyde, Nucl. Phys. **A651**, 323 (1999).
[32] L. L. Riedinger, N. R. Johnson, and J. H. Hamilton, Phys. Rev. **179**, 1214 (1969).
[33] J.-Y. Zhang, M. A. Caprio, N. V. Zamfir, and R. F. Casten, Phys. Rev. C **60**, 061304(R) (1999).
[34] E. der Mateosian and J. K. Tuli, Nucl. Data Sheets **75**, 827 (1995).
[35] C. W. Reich and R. G. Helmer, Nucl. Data Sheets **85**, 171 (1998).
[36] R. G. Helmer, Nucl. Data Sheets **77**, 471 (1996).
[37] R. F. Casten and N. V. Zamfir, Phys. Rev. Lett. **87**, 052503 (2001).
[38] R. M. Ronningen, R. S. Grantham, J. H. Hamilton, R. B. Piercey, A. V. Ramayya, B. van Nooijen, H. Kawakami, W. Lourens, R. S. Lee, W. K. Dagenhart, and L. L. Riedinger, Phys. Rev. C **26**, 97 (1982).
[39] D. Ward, H. R. Andrews, O. Häusser, Y. El Masri, M. M. Aléonard, I. Yang-Lee, R. M. Diamond, F. S. Stephens, and P. A. Butler, Nucl. Phys. **A332**, 433 (1979).
[40] H. Emling, E. Grosse, R. Kulessa, D. Schwalm, and H. J. Wollersheim, Nucl. Phys. **A419**, 187 (1984).
[41] G. Böhm, A. Dewald, P. Petkov, and P. von Brentano, Nucl. Instrum. Methods Phys. Res. A **329**, 248 (1993).